Western Michigan University
ScholarWorks at WMU

Master's Theses

Graduate College

12-2003

Color Management of Desktop Input Devices: Quantitative Analysis of Profile Quality

Xiaoying Rong

Follow this and additional works at: https://scholarworks.wmich.edu/masters_theses

 Part of the Construction Engineering and Management Commons

Recommended Citation

Rong, Xiaoying, "Color Management of Desktop Input Devices: Quantitative Analysis of Profile Quality" (2003). *Master's Theses*. 4760.
https://scholarworks.wmich.edu/masters_theses/4760

This Masters Thesis-Open Access is brought to you for free and open access by the Graduate College at ScholarWorks at WMU. It has been accepted for inclusion in Master's Theses by an authorized administrator of ScholarWorks at WMU. For more information, please contact wmu-scholarworks@wmich.edu.

COLOR MANAGEMENT OF DESKTOP INPUT DEVICES: QUANTITATITIVE ANALYSIS OF PROFILE QUALITY

by

Xiaoying Rong

A Thesis
Submitted to the
Faculty of The Graduate College
in partial fulfillment of the
requirements for the
Degree of Master of Science
Department of Paper Engineering, Chemical Engineering and Imaging

Western Michigan University
Kalamazoo, Michigan
December 2003

Copyright by
Xiaoying Rong
2003

ACKNOWLEDGMENTS

First, I would like to thank my advisors Dr. Dan Fleming and Dr. Abhay Sharma for guiding me to finish this thesis. Thanks for showing me the new technology in the graphic arts industry that I have been working on for over seven years. Thanks for your encouragement.

Next, I would like to thank Ms. Lois Lemon for all the good times we worked together as your teaching assistant and as friends.

Finally, I would like to thank my parents, Xiuling Cao and Zhongqi Rong, for supporting and encouraging me at all times. I would like to thank my husband Xi Shen for your love.

Xiaoying Rong

COLOR MANAGEMENT OF DESKTOP INPUT DEVICES: QUANTITATIVE ANALYSIS OF PROFILE QUALITY

Xiaoying Rong, M.S.

Western Michigan University, 2003

This thesis investigates the color management principle and input device profiling. The input devices discussed in this thesis are flatbed scanners.

In this thesis, the human visual system, CIE L*a*b* color space, ICC profiles are reviewed, and the evaluation of profile quality is discussed. Grayscale and standard color targets of three primary suppliers are used to create profiles for a scanner. The quantitative analyses of the quality of different profiles, created by two primary commercial profiling software, are conducted according to the Delta-E of the CIE L*a*b* color space. Finally, the relationship of different color targets and profiles for desktop input color management are discussed.

TABLE OF CONTENTS

Table of Contents—continued

LIST OF TABLES

List of Tables—continued

LIST OF FIGURES

List of Figures—continued

I. INTRODUCTION

The concept of color management has been incorporated into the printing industry for many years. The typical workflow of reproducing color consists of capturing images by scanners, digital cameras, displaying images on monitors, proofing and printing on press. In closed-loop color reproduction, the color reproduction characteristics of the output device are used to adjust scanner settings, "closing the loop" between input and output devices. In open-system color, a device-independent color space is used as an intermediate step [1, 2]. With the device-independent color space, the operators of scanners, printers or presses do not need to know the characteristics of other devices. The image files with devices' characteristics can explain how the colors are rendered in a device-independent color space. With the introduction of color management, it is possible to have a variety of sources for color images, all open platforms along with a variety choice of output devices. The quality of color images can be predictably controlled. The solution is implementation of a Color Management System (CMS).

Professional workflow without color management is not conceivable anymore. Since every input and output device has its own color gamut, one cannot assume colors to be consistent when transforming from device to device. This is where a CMS becomes relevant. A dedicated ICC (International Color Consortium) profile has to be generated for every input and output device, in order to describe their color space behavior. Within the workflow, the Color Management System compares the profiles of the data sender, i.e., a scanner, with the profile of the data receiver, i.e., a

monitor, and calculates a relation for the conversion, which will translate the image data into the right color impression [3].

To achieve high image quality throughout a digital imaging system, the first requirement is to ensure the quality of the devices that capture real-world physical images and convert to digital images. For example, desktop scanners and digital cameras can digitize original pictures and scenes. Scanners and digital cameras as the input devices, are now affordable for everybody. As the source of capturing color images in the real world, scanners and digital cameras play an important role in the color reproduction workflow. Without predictable capture and accurate color space rendering, it is impossible to get the correct color display and reproduction, even with a profiled monitor and printer.

II. THE HUMAN VISUAL SYSTEM AND CIE STANDARD OBSERVERS

In the human vision system, when the eye is properly focused, light from an object outside the eye is imaged on the retina. Pattern vision is afforded by the distribution of discrete light receptors over the surface of the retina. The retina contains two main types of light-sensitive cells, the rods and cones. Cod vision is called photopic or bight-light vision. Rods serve to give a general, overall picture of the field of view. They are not involved in color vision and are sensitive to low levels of illumination. This is known as scotopic or dim-light vision. There are three types of cones, named L, M, S, which are sensitive mainly to light containing long, middle and short wavelengths, respectively (Figure 1) [4].

Four concepts are used to understand the human visual system: spectral sensitivity, opponent encoding, spatial resolution and nonlinear response. Incident

light interacts with visual receptors, rods and cones. Following a chemical reaction, light energy is converted to a neural signal [5].

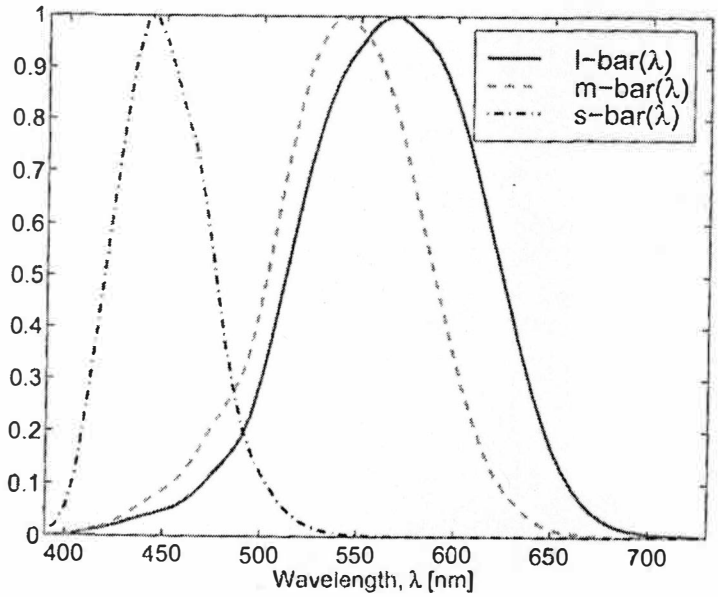

Figure 1: Normalized spectral sensitivity curves l(λ), m(λ), and s(λ), of the three different types of cones, L, M, S, responsible for photopic vision, according to color science [5]

Spectral sensitivity defines a detector's sensitivity as a function of wavelength. Because there are only three types of cones and their spectral sensitivities are overlapping, many different objects can produce the same cone responses, leading to identical appearing color. That is why it is possible that small numbers of colorants can reproduce our world, comprised of thousand of colorants.

The cones combine spatially and form opponent signals, white/black, red/green, and yellow/blue. It is not possible to have a color that is simultaneously reddish and greenish.

Spatial resolution defines the resolving power of an imaging system and leads to the ability to discern fine detail. The black/white signal has the highest spatial

resolution, followed by the red/green signal. The yellow/blue signal has quite low spatial resolution.

The complex signal processing of the human visual system results in a nonlinear (curved) relationship between light imaged onto the eye and resulting color perceptions. This means that for dark colors, small changes in an object's reflectance or transmittance lead to large changes in lightness. For light colors, the opposite occurs [5].

In 1931, the International Commission of Illumination (CIE) defined a standard observer. These standard observer data consist of color matching functions obtained with the monochromatic primaries of wavelengths $R_0=700nm$, $G_0=546.1nm$, and $B_0=435.8nm$ for the reference equienergetic white E. The following functions define the CIE Standard RGB Colorimetric System and the CIE 1931 Standard XYZ Colorimetric System [6].

$$R = \int_{\lambda_{min}}^{\lambda_{max}} f(\lambda)\bar{r}(\lambda)d\lambda \quad (1)$$

$$G = \int_{\lambda_{min}}^{\lambda_{max}} f(\lambda)\bar{g}(\lambda)d\lambda \quad (2)$$

$$B = \int_{\lambda_{min}}^{\lambda_{max}} f(\lambda)\bar{b}(\lambda)d\lambda \quad (3)$$

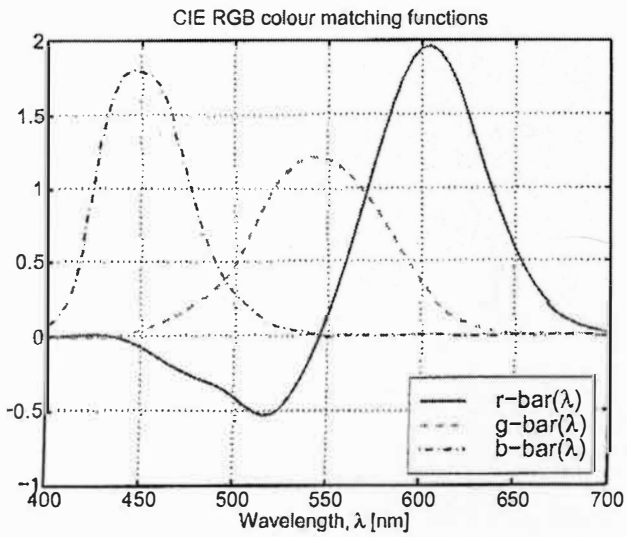

Figure 2: CIE color matching function of $\bar{r}(\lambda)$, $\bar{g}(\lambda)$, $\bar{b}(\lambda)$ [6]

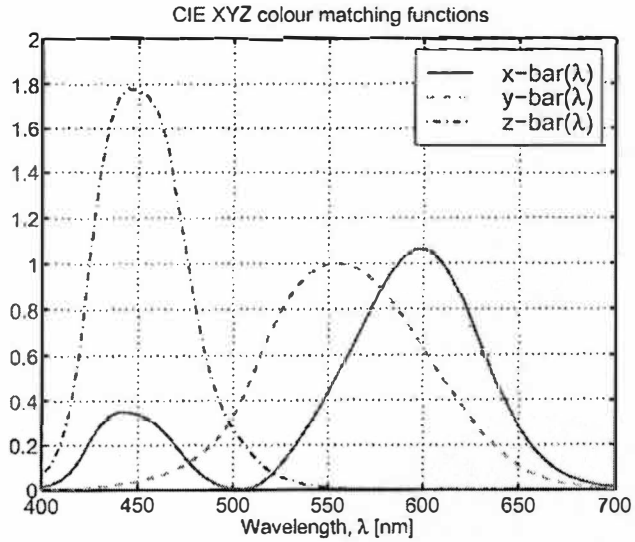

Figure 3: CIE color matching function of CIE 1931 2° standard observer [6]

$$X = \int_{\lambda_{min}}^{\lambda_{max}} f(\lambda)\bar{x}(\lambda)d\lambda \tag{4}$$

$$Y = \int_{\lambda_{min}}^{\lambda_{max}} f(\lambda)\bar{y}(\lambda)d\lambda \tag{5}$$

$$Z = \int_{\lambda_{min}}^{\lambda_{max}} f(\lambda)\bar{z}(\lambda)d\lambda \tag{6}$$

where: $f(\lambda)$ is the spectral radiant power distribution of a given color stimulus. $\bar{r}(\lambda)$, $\bar{g}(\lambda)$, $\bar{b}(\lambda)$ are color matching functions, and they define the tristimulus value of the spectrum colors for this particular set of primaries. $\bar{x}(\lambda)$, $\bar{y}(\lambda)$, $\bar{z}(\lambda)$ are CIE color matching functions of the 2° 1931 CIE standard observer.

X, Y, Z are all positive and the value of Y is proportional to the luminance of the given color.

A mathematical model was derived by the CIE in 1976 [7], known as CIE L*a*b*, or its official abbreviation CIELAB. The coordinates, L*, a*, and b* represent the perception of lightness, redness/greenness, and yellowness/blueness, respectively. The coordinates are calculated from the knowledge of an object's spectral reflectance or transmittance properties, a light source interacting with an object, and the spectral sensitivities of an observer.

III. COLOR SPACES AND COLOR DIFFERENCES

RGB Color Space

Most of the devices for capturing images have an LMS-fashion light detector [8]. L, M, and S are referred to as long, middle and short wavelength sensitivity which were descried in the previous chapter. The color is described with three components: R, G, and B. The value of these components is the sum of the respective sensitivity functions and the incoming light, which can be described by the following equations:

$$R = \int_{300}^{830} S(\lambda)R(\lambda)d\lambda \tag{7}$$

$$G = \int_{300}^{830} S(\lambda)G(\lambda)d\lambda \tag{8}$$

$$B = \int_{300}^{830} S(\lambda)B(\lambda)d\lambda \tag{9}$$

$S(\lambda)$ is the light spectrum, and $R(\lambda)$, $G(\lambda)$ and $B(\lambda)$ are the sensitivity functions for the R, G and B sensors, respectively.

The equations show that the RGB values depend on specific sensitivity functions of the capture devices. The sensitivity functions for the R, G, B channels may differ from device to device. This makes RGB color space a device-dependent color space. Another problem is the perceptual non-uniformity, which means a low correlation between the perceptual difference of two colors and the Euclidian distance in RGB color space.

CMY(K) Color Space

Desktop printers which are either CMY(cyan, magenta, yellow) or CMYK(cyan, magenta, yellow, and black), reproduce color based on subtractive color mixing.

In contrast to additive mixing of colors, which occurs on self-luminous displays, subtractive mixing of colors is a way to produce colors by selectively removing a portion of the visual spectrum [9]. Subtractive color mixing depends on dyes or pigments at the surface. The more dyes or pigments the less reflected light. The subtractive color mixing is complex. It depends on dyes or pigments and the relationship between them and the medium.

The CIE 1976 L*a*b* Space

In 1976, the CIE proposed CIEL*a*b* color space to provide a perceptually uniform color space [10]. This means that the Euclidian distance between two colors in the CIEL*a*b* color space is strongly correlated with human visual perception.

The CIE L*a*b* is a three-dimensional plot calculated from CIEXYZ tristimulus values, in which L* is the luminance, a* is the red-green axis, and b* is the blue-yellow axis.

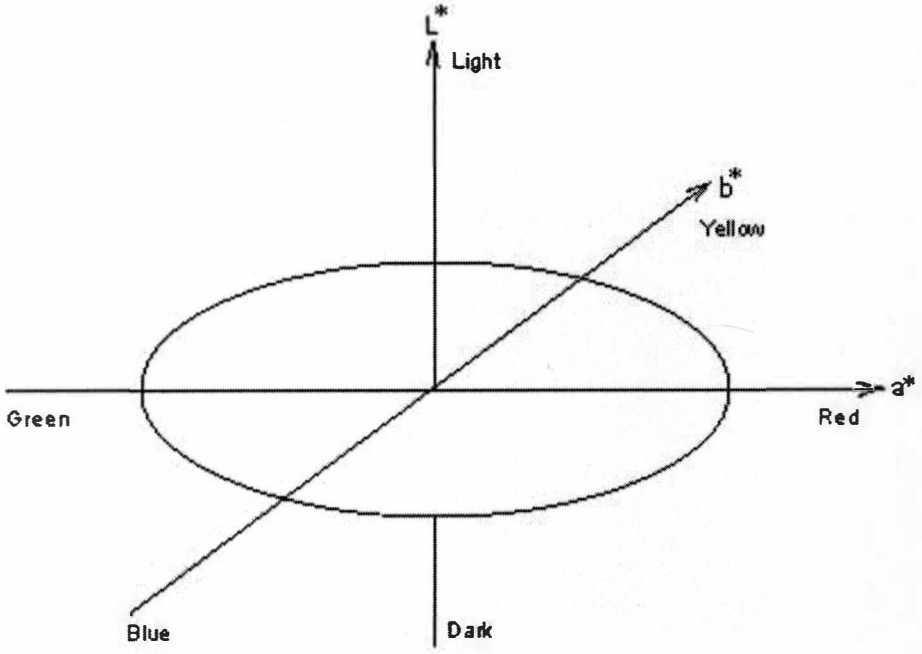

Figure 4: The CIEL*a*b* color space

The CIE L*a*b* (CIELAB) values are defined by the following equations [7]:

$$L^* = 116 f\left(\frac{Y}{Y_n}\right) - 16 \tag{10}$$

$$a^* = 500\left[f\left(\frac{X}{X_n}\right) - f\left(\frac{Y}{Y_n}\right) \right] \tag{11}$$

$$b^* = 200\left[f\left(\frac{Y}{Y_n}\right) - f\left(\frac{Z}{Z_n}\right) \right] \tag{12}$$

Where $f(t) = f(t)^{1/3}$ for $t > 0.008856$ and $f(t) = 7.78(t) + \frac{16}{116}$ for $f \le 0.008856$; while $f(t)$ as a single valued function of t.

X, Y, and Z are defined by equation (4), (5) and (6). X_n, Y_n, Z_n are tristimulus values of the reference white.

The formulas for L*, a*, and b* contain cube roots and thus known as nonlinear transformations.

The tristimulus values X_n, Y_n, Z_n are those of the nominally white stimulus. For the example for illuminant D_{50}, the values are calculated as the following (color spaces):

$$Y_n = \int_{\lambda_{min}}^{\lambda_{max}} 1 \cdot l_{D50}(\lambda) \cdot \bar{y}(\lambda) d(\lambda) = 96.42 \tag{13}$$

$$X_n = \int_{\lambda_{min}}^{\lambda_{max}} 1 \cdot l_{D50}(\lambda) \cdot \bar{x}(\lambda) d(\lambda) = 100.00 \tag{14}$$

$$Z_n = \int_{\lambda_{min}}^{\lambda_{max}} 1 \cdot l_{D50}(\lambda) \cdot \bar{z}(\lambda) d(\lambda) = 82.49 \tag{15}$$

The reverse transformation (for X/X_n, Y/Y_n, $Z/Z_n > 0.008856$) is

$$X = X_n\left(\frac{L^*+16}{116} + \frac{a^*}{500}\right)^3 \tag{16}$$

$$Y = Y_n\left(\frac{L^*+16}{116}\right)^3 \tag{17}$$

$$Z = Z_n\left(\frac{L^*+16}{116} - \frac{b^*}{200}\right)^3 \tag{18}$$

L* represents the lightness of a color, known as the CIE 1976 psychometric lightness. The scale of L* is 0 to 100. 0 represents the ideal black and 100 represents the reference white.

The CIE 1976 chroma is designated by the distance from L* axis as

$$C^*_{ab} = \sqrt{a^{*2} + b^{*2}} \tag{19}$$

The CIE 1976 hue angle is defined as

$$h_{ab} = \arctan\left(\frac{b^*}{a^*}\right) \tag{20}$$

Figure 5 plots The a*-b* plane of CIELAB color space.

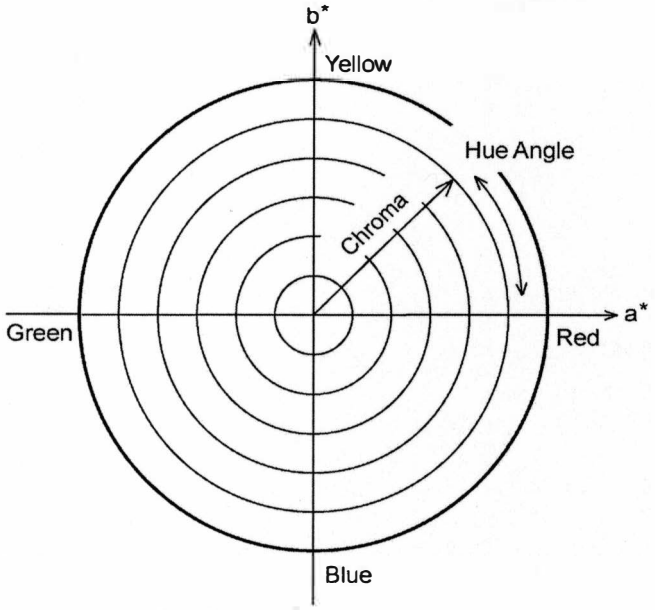

Figure 5: a*-b* plane of CIELAB color space

Color Difference

CIELAB color values are often used in the graphic arts industry for color reproduction quality control, such as comparing the color differences of printed reproduction and original item. The CIE color difference can also be used to measure the difference between images captured by scanners, digital cameras and the originals.

Delta-E (ΔE), a measure of color differences in CIELAB space, is calculated using the distance formula to determine the distance in color space from one color to another based on the CIE 1976 L*a*b* color space [7].

$$\Delta E^*_{ab} = \sqrt{(L^*_2 - L^*_1)^2 + (a^*_2 - a^*_1)^2 + (b^*_2 - b^*_1)^2} \tag{21}$$

where:

L_1*, a_1*, b_1* = CIELAB coordinates of reference color

L_2*, a_2*, b_2* = CIELAB coordinates of comparison color

In the a*b* plane, the radial distance $\sqrt{a^{*2} + b^{*2}}$ and angular position $\arctan\left(\frac{b^*}{a^*}\right)$ correlate chroma and hue angle, respectively as shown in equations (19) and (20).

Many users of color difference equations attempt to use only one color difference value, which is ΔE. This procedure will not relate to visual assessment. There are three aspects to the perception of color, which are hue, saturation, and lightness. These three do not have equal effect on visual perception of the acceptability of color. Often the concept of hue is more critical than either saturation or lightness. If a color has correct hue, it can be off in saturation or lightness and still be visually acceptable [10].

ΔE_{ab}*, ΔH_{ab}* and ΔC_{ab}* are very useful to compare two colors in CIELAB color space. ΔH* indicates the effective hue difference in CIELAB color difference analysis. ΔC_{ab} indicates the chroma (saturation) difference.

$$\Delta C^*_{ab} = C^*_2 - C^*_1 = \sqrt{a^{*2}_2 + b^{*2}_2} - \sqrt{a^{*2}_1 + b^{*2}_1} \tag{22}$$

$$\Delta H^*_{ab} = \sqrt{\left(\Delta E^*_{ab}\right)^2 - \left(\Delta L^*\right)^2 - \left(\Delta C^*_{ab}\right)^2} \tag{23}$$

ΔH^*_{ab} is assigned a positive value when Δh_{ab} is positive and assigned a negative value when Δh_{ab} is negative.

The total color difference, which is represented by ΔE_{ab}^{*} in CIE terminology, is correlated with visual judgments of color difference, but is not perfect. Once the total color difference is calculated, information about the direction of color error, which is much more important than the total magnitude of error, is lost also [10].

It has been found that the CIELAB space is not completely uniform. The color difference ΔE_{ab}* is not perfect. Several attempts have been made to define better color difference formulae, e.g., CMC (l:c), BFD, CIE94 and CIE2000.

The weighted color difference *ΔE94* has been introduced referred to CIE94. The equation was designed for industries manufacturing colored products [11]. The weight is optimized to improve correlation with visual tolerances.

$$\Delta E_{94}^{*} = \sqrt{\left(\frac{\Delta L^{*}}{k_L S_L}\right)^2 + \left(\frac{\Delta C^{*}}{k_C S_C}\right)^2 + \left(\frac{\Delta H^{*}}{k_H S_H}\right)^2} \qquad (24)$$

The weighting functions, S_L, S_C and S_H, vary with the chroma of the reference specimen C^* as following,

$S_L=1$, $S_C=1+0.045C^*$, $S_H=1+0.015C^*$

The variables k_L, k_C and k_H are called parametric factors and are included in the formula to allow for adjustments to be made independently for each color difference. Under the reference conditions, $k_L=k_C=k_L=1$.

IV. ICC-BASED COLOR MANAGEMENT SYSTEM AND DESKTOP INPUT DEVICES

ICC-Based Color Management System

With the flexibility of digital technology, digitized images are often transformed between input and output devices. Every device has a difference color

gamut, which affects the quality and color accuracy of the reproduction. The solution is the implementation of a Color Management System (CMS) [1, 2].

A color gamut is the range of color that any given device can detect, display or print. If the source device contains colors that cannot be recognized or reproduced by the receiving device, the color gamut needs to be compressed and out-of-gamut colors are replaced with the nearest possible achievable colors [12]. In the open platform, color reproduction workflow starts and ends at different sites. Therefore, colors must be described in such a way that all devices interpret it correctly. That is why the International Color Consortium (ICC) developed a standard, device-independent color definition based on CIE color spaces [13]. Basically, a profile is created for each device, which maps its device-independent color values to an object color space, such as CIELAB. Color Management Modules (CMMs) combine profiles into device-to-device color transformations, which translate the CIELAB values into a color space of a device (e.g., RGB for scanners, monitors, digital cameras; CMYK for printers, etc.) [13].

Device profiles provide a color management system with the information necessary to convert color data between native device color spaces and device independent color spaces. The framework of color management is illustrated in the ICC Specification (Figure 6) [13].

Device profiles defined by the ICC specifications store colorimetric information of color imaging devices and can be used to translate color created in one device into another device's native color space. CMMs will receive both image data and source or destination device profiles from the applications or device driver. CMMs firstly use the source profile to convert input image data to intermediate

device independent color space, and then use the destination profile to convert intermediate color space to an output device's native color space.

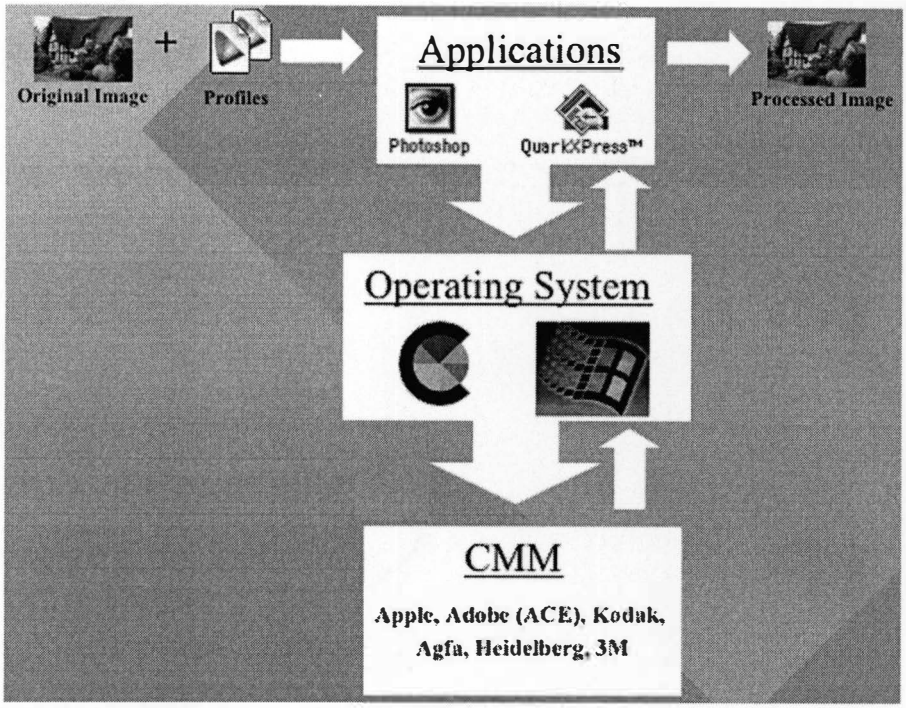

Figure 6: Color management architecture [2]

A key component of these profiles is a well defined profile connection space (PCS). [13] In general, the actual device gamut will not be large enough to reproduce the desired color appearances communicated by the PCS values. Four rendering intents, also known as gamut mapping styles, are provided to address this problem. The rendering intents are media-relative colorimetric intent, ICC-absolute colorimetric intent, perceptual intent, and saturation intent.

The media-relative colorimetric intent is a rendering intent method that maps the white point of the source image to a destination device. It is useful for colors that have already been mapped to a medium with a smaller gamut than the reference medium and need no further compression. Any of the source image colors that fall

outside the gamut of the output device are clipped to the nearest in gamut color values.

The ICC-absolute colorimetric intent is a rendering method that maps the white point and black point of the source image to the white point and black point of the destination device. It is useful for the spot color and when simulating one medium on another.

The perceptual intent is a rendering method that maps or compresses the colors from the source image to the colors of the destination device, while maintaining the overall appearance of the image. This intent can be explained as trading off preservation of contrast to preserve detail through the tonal range. It is useful for general reproduction of images, particularly pictorial or photographic-type images.

The saturation intent is a rendering method that maps saturated colors of the sourced image to the saturated colors of the destination device. This intent can be explained as trading off preservation of hue to preserve the vividness of pure colors. It is useful for images which contain object such as charts or diagrams.

Desktop Color Input Device- Flatbed Scanner

Scanners are usually designed for scanning images reproduced on paper or transparencies and include their own source of illumination. Color digitizing scanners, which produce RGB output, are important components of desktop color publishing systems. Compared to the high-end scanners, they offer advantages in compactness, low price, and ease of use [14].

Scanners vary in resolution and sharpness. The scanner's resolution is determined by the number of sensors in a single row (x-direction sampling rate) of the

CCD (charged couple device) array by the precision of the stepper motor (y-direction sampling rate). Sharpness depends mainly on the quality of the optics used to make the lens and the brightness of the light source. Interpolation is a process that the scanning software uses to increase the perceived resolution of an image. It does this by creating extra pixels between adjacent pixels. It is not a hardware resolution. The bit depth refers to the numbers of colors that the scanner is capable of reproducing. Each pixel requires at least 24-bits to create a true color [14].

The schematic of a color scanner is given in Figure 7.

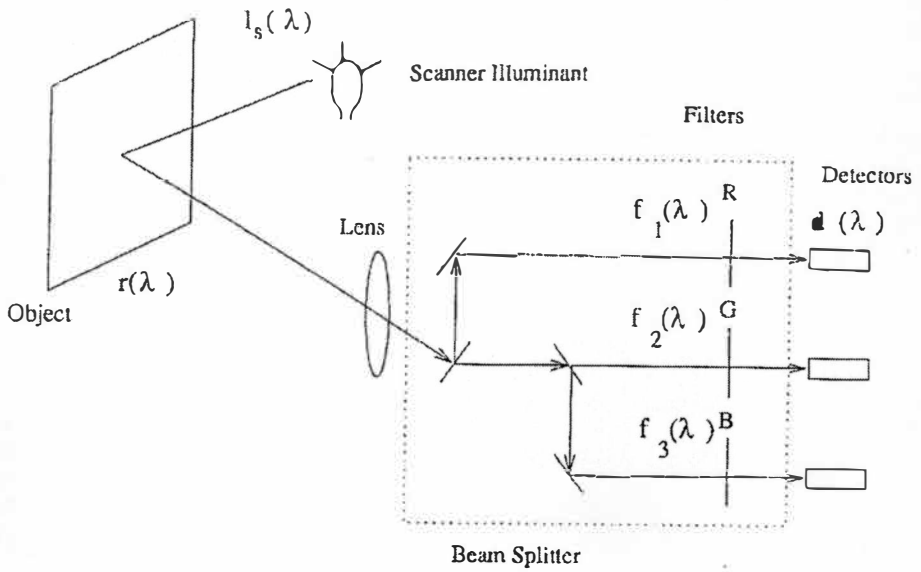

Figure 7: Schematic of a color scanner [15]

The imaging sensor used in most scanners is the CCD. A CCD imaging sensor starts at the point of converting light (photons) into electrons. The next step is to read the value (accumulated charge) of each cell in the image. CCD sensors can create high quality, low noise images. Picture quality is strictly related to the number of pixels composing the sensor, the higher the better [16].

For color accuracy, the most important characteristic of the imaging sensor is its spectral sensitivities. Ideally, they should closely resemble the human visual system's spectral sensitivities [5].

The raw CCD sensor signals, in the form of analog signals are amplified and digitized using an analog-to-digital converter (ADC). The range of digital values depends on the number of bits in the ADC. Most commonly, 8, 12, or 16-bit ADC's are used [16].

If scanners are designed to be colorimetric, a transformation, independent of the scanned object's characteristics, can be used to accurately estimate the CIEXYZ tristimulus values from the scanner measurements [15]. A well-calibrated and profiled scanner is able to convert the output RGB values into device-independent color coordinates, such as CIELAB.

V. SCANNER CALIBRATION AND CHARACTERIZATION

Many color device calibration tasks involve transporting device dependent color, which may be RGB or CMYK, to device independent color space, which may be CIEXYZ or CIELAB. The mathematical model is usually built to correlate the coordinates of device and CIE colorimetry.

Typically, color reproduction starts with capture of an image by digital cameras or scanners. The captured image is displayed on a monitor, edited, and then output to a conventional printing press, digital press, or proofer.

Scanner calibration refers to adjustment of the response of the scanner's light detectors so that the detectors consistently record specified digital values for given densities in the original, and all detectors record the same digital value [1]. With the

CCD scanner, it may also mean compensating for any non-uniformity in sensitivity of the individual element of the array [17].

Scanner characterization provides a way of determining the digital color values output by the scanner in response to specified colors in an original. It defines the relationship between the device dependent color space to the CIE color space. For a scanner or camera, it normally defines the relationship between the voltages quantized as data recorded on the disk and the CIE measurements of the colors scanned [17]. Characterization is affected by such variables as the scanner's dynamic range of densities it can detect, from lightness to darkest; how the scanner renders contrast, as measured by gamma; whether the scanner reproduces neutral colors as neutral [1].

Scanner characterization can be conveniently achieved by using ANSI IT8.7/2 [18] as a reflection target. The primary target suppliers are Eastman Kodak, Fuji Film, and Agfa.

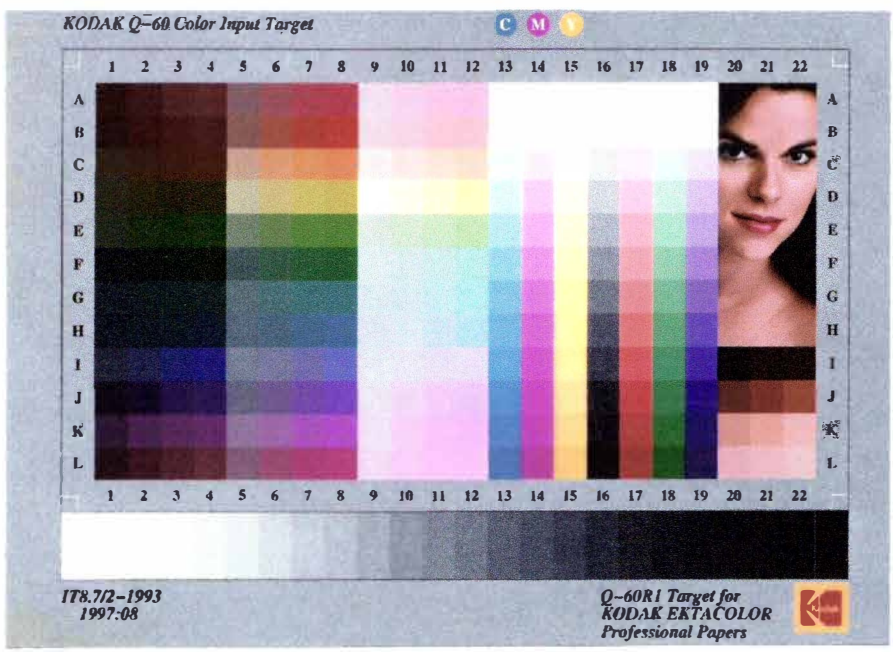

Figure 8: Kodak IT8.7/2 target for input device

IT8.7/2 is designed to help the scanner operators establish the basic tone reproduction and color correction set up for various family products. The target design provides uniform mapping in the CIELAB color space and is defined in detail in ANSI standard IT8.7/1 [19] for transmission materials and IT8.7/2 [18] for reflection materials. Both targets are based upon a similar concept that uses twelve hue angles (rows A-L) and three lightnesses at each hue angle. At each hue angle and lightness combination, there are four chroma or saturation levels. The fourth chroma (columns 4, 8, and 12) represents the maximum chroma (colorfulness) that the specific product can produce at that hue angle and lightness level. Columns 13-19 contain cyan, magenta, yellow, neutral, red, green and blue scales. The neutral scale is defined to begin at neutral D-min and end at neutral D-max in 12 steps with equal lightness (L*) increments. Across the bottom of the target, there is a 22 step neutral scale. Hue can be specified as the angle, and chroma can be specified as C*. Target values are shown in the following table. The C4 values are targeted to be the largest value achievable on the given photo paper at a given hue angle and L* value.

Row	Hue Angle	L1	C1	C2	C3	C4	L2	C1	C2	C3	C4	L3	C1	C2	C3	C4
Column			*1*	*2*	*3*	*4*		*5*	*6*	*7*	*8*		*9*	*10*	*11*	*12*
A	16	20	12	25	37		40	15	30	44		70	7	14	21	
B	41	20	12	24	35		40	20	36	54		70	8	16	24	
C	67	24	11	21	32		55	22	44	66		75	10	20	30	
D	92	25	10	19	29		60	20	40	60		80	10	21	31	
E	119	25	11	21	32		45	16	32	48		70	9	18	27	
F	161	15	9	19	28		35	14	28	42		70	6	12	18	
G	190	20	10	20	30		40	13	25	38		70	6	13	19	
H	229	20	9	18	27		40	12	24	36		70	7	13	20	
I	274	25	12	24	35		45	9	19	28		70	5	10	15	
J	299	15	15	29	44		40	11	22	33		70	6	11	17	
K	325	25	16	33	49		45	14	28	42		70	8	15	22	
L	350	20	13	26	38		40	16	32	48		70	8	15	22	

Table 1: Common L* and C* values vs. hue angle for reflection targets [18]

Commercial profiling software are used to compare the raw scanned CIELAB values to the reference value of the target and to create profiles for a certain scanner. The most popular profile software are Gretag ProfileMaker, Monaco Profiler and Fuji ColourKit ProfileMaker. Different software usually produce similar results [21, 22]. Significant differences may occur in using software whose profiles use different color management modules (CMMs). Different scanner profiling software can be evaluated by comparing the ΔE_{ab}^{*}, ΔH_{ab}^{*} and ΔC_{ab}^{*}. A grayscale can be used to evaluate the color balance [20].

VI. EXPERIMENTAL

Profiling software and standard color targets are widely used in almost all color reproduction areas, such as the graphic arts industry, photography, and digital libraries. The usage of profile software and standard color targets makes color reproduction easier to be controlled.

Color targets for scanners are supplied by the primary film and photo paper manufacture covered in ISO 12641 [18]. Different targets from difference manufacture have different CIELAB values. The users usually use a certain target and certain profiling software. This brings the question to the accuracy of the profile created by one profiling software using one target. Here we present a test of two primary profile software packages using three different color targets to find a correlation for different combinations.

Scanner Testing

Before starting to profile the scanner, some properties need to be tested, such as dynamic range and gray balance. The desktop flatbed scanner used was an HP Scanjet 7400C. A Stouffer® R1215 12 step grayscale was scanned to test the dynamic range and gray balance.

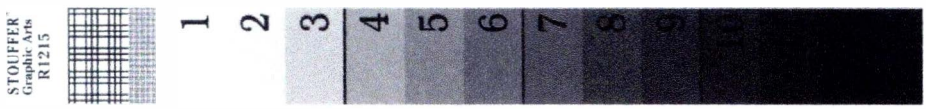

Figure 9: Stouffer R1215 12 step grayscale

The following figure shows the R(red), G(green) and B(blue) digital values from the scanned grayscale.

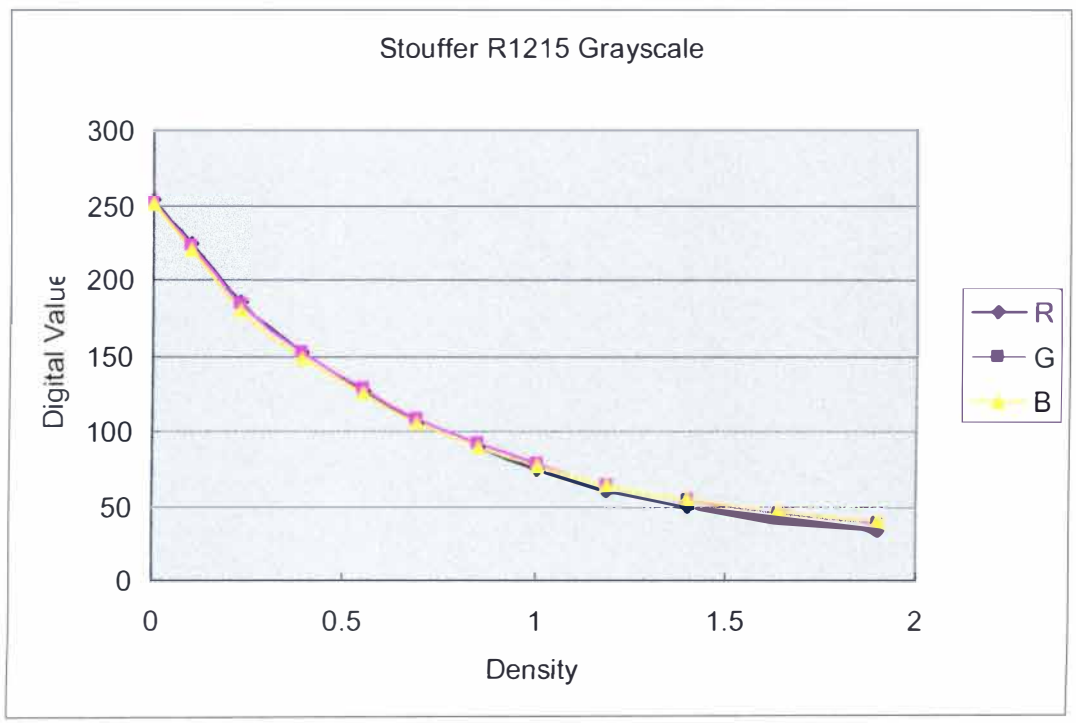

Figure 10: RGB digital values of Stouffer R1215 grayscale scanner by HP Scanjet 7400C with no auto adjustment

Figure 10 shows that HP Scanjet 7400C has high dynamic range and good unadjusted gray balance in highlight and midtone area, and a small shift in the shadow area of Red.

Figure 11 shows the measured a* and b* values of R1215 grayscale, which were measured by a Gretag Macbeth Spectrolino with Monaco Measure Tool at D_{50} 2°.

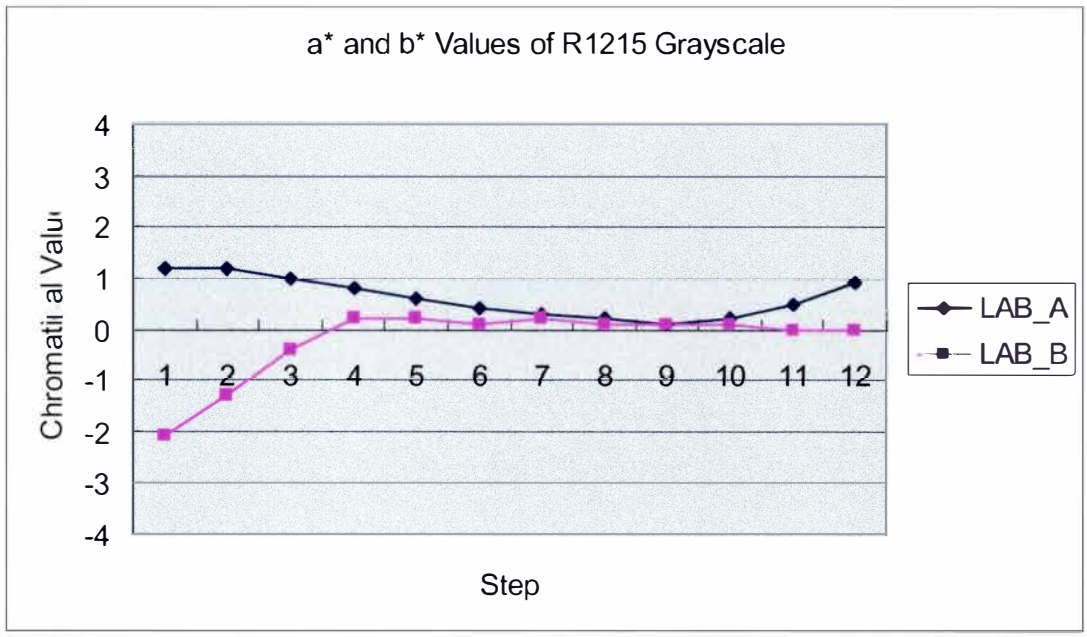

Figure 11: Measured a* and b* values of Stouffer R1215 grayscale

Most of the desktop flatbed scanners have auto exposure and auto color adjustment function. To get the raw digital value of the scanner, all auto adjustment functions have been turned off.

The R1215 grayscale and Kodak color target were scanned in three difference ways to test the auto exposure function. Figures 12, 13 and 14 show the results of three difference tests.

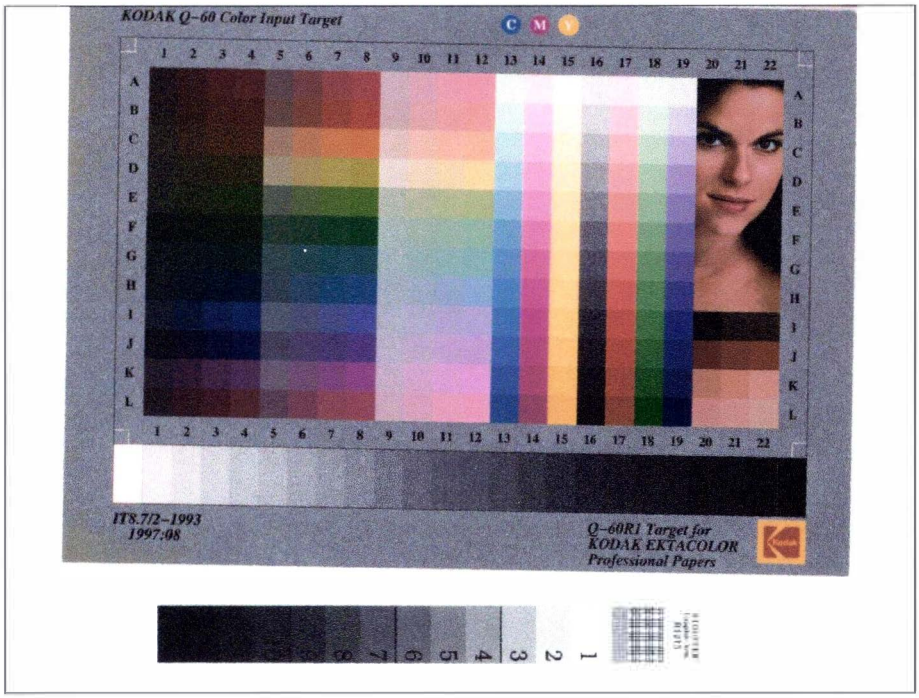

Figure 12: Target and grayscale are scanned at the same time with a certain select area

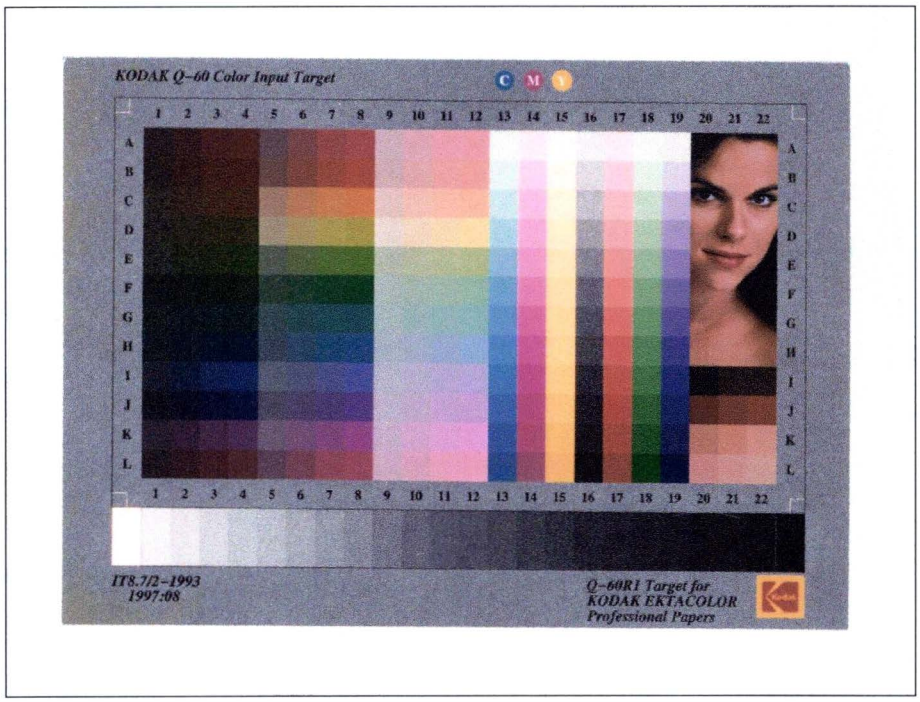

Figure 13: Scanned color target only with the same selected area as Figure 12

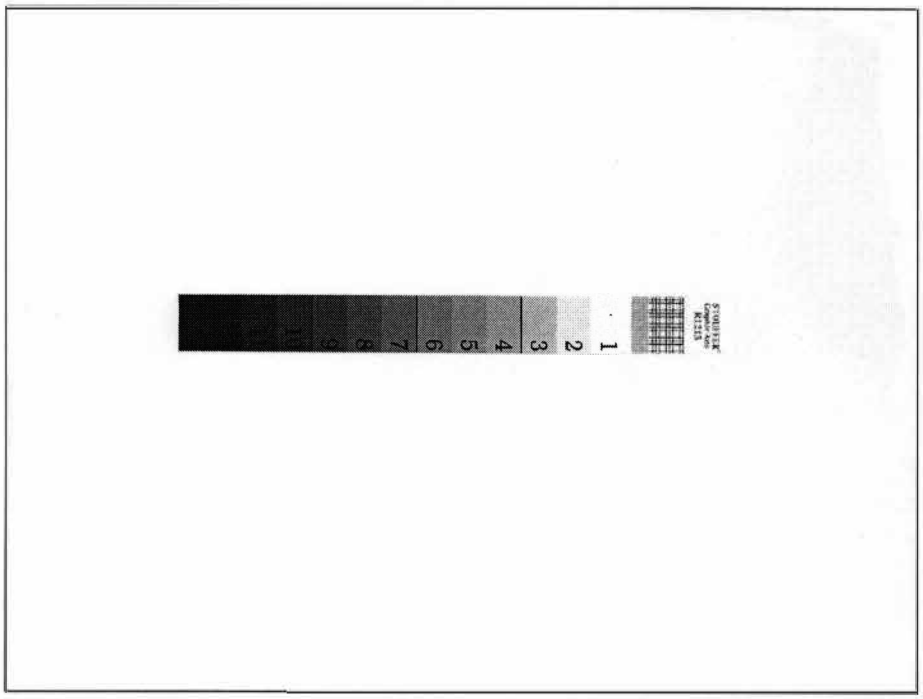

Figure 14: Scanned grayscale only with the same selected area as Figure 12

The D_{min}, D_{max}, and three other points of R, G, B values of grayscales on three testing have been measured to check the auto adjustment function of the scanner. The data are listed in Table 2 and Table 3.

Figure	Steps	Dmin	5	10	15	Dmax
Figure 10	R	247	172	111	67	25
	G	240	169	111	68	34
	B	237	168	112	70	32
	Steps	**Dmin**	**5**	**10**	**15**	**Dmax**
Figure 11	R	248	172	112	68	25
	G	241	170	11	68	32
	B	234	169	113	71	32

Table 2: RGB values of grayscale on Kodak08 from Figure 10 and Figure 11

Figure	Steps	1	3	6	9	12
Figure 10	R	253	185	106	60	32
	G	252	184	109	65	38
	B	251	180	106	64	39
	Steps	**1**	**3**	**6**	**9**	**12**
Figure 12	R	253	185	107	61	33
	G	252	185	110	65	39
	B	251	180	107	64	40

Table 3: RGB values of Stouffer R1215 grayscale of Figure 10 and Figure 12

The data in the tables showed that the RGB values are very close. It means when the auto adjustment function is turned off no adjustment has been made no matter the size of selected area.

The Difference of Measured and Reference CIELAB Values of Three Targets

Every color target has its own reference CIELAB values supplied by the manufacture. The actual CIELAB values were measured by a Gretag Macbeth SpectraScanT using MeasureTool software to compare the difference of measured data and reference data. CIELAB values of scanned image were read by using our own program [21, 22].

The reference data of Kodak targets has the standard deviation for customer to verify if the difference is in the tolerance range. According the reference data supplied by Eastman Kodak, the average standard deviation of Delta E on Kodak 08 is 0.41. This means if the measured Delta E is equal or smaller than 0.41, the profile created by using this target is as reliable as the target itself. The measured and calculated data showed that the standard deviation of Kodak08 is 1.31 which is larger than the

reference one. This relatively small variation might come from the aging effect of the emulsion.

Table 4 shows the color difference of measured data and reference data, RMS means root mean square.

Color Targets	Agfa	Fuji	Kodak08
RMS DeltaE	1.44	2.25	3.73
Maximum Delta E	3.13	6.18	6.35
Average Delta E	1.32	1.92	3.5
RMS Delta L*	0.63	0.93	0.45
RMS Delta a*	0.72	1.29	2.12
RMS Delta b*	1.08	1.59	3.04
Standard Deviation of Delta E	0.59	1.18	1.31

Table 4: Color difference of three targets—comparison of reference data and measured data

Data in the Table 4 shows that the Agfa target has a smaller RMS Delta E value than the other two targets. Kodak08 has the largest difference. The contour of Delta E values on Kodak08 is shown in Figure 15.

Figure 15 shows that columns 14 and 19 have the larger Delta E values. This means that patches of magenta on the Kodak target have larger Delta E values. This can be caused by an aging effect and a variety of emulsions.

The difference of reference data and measured data will affect the accuracy of the profile when the profile is created by using the reference data of the target.

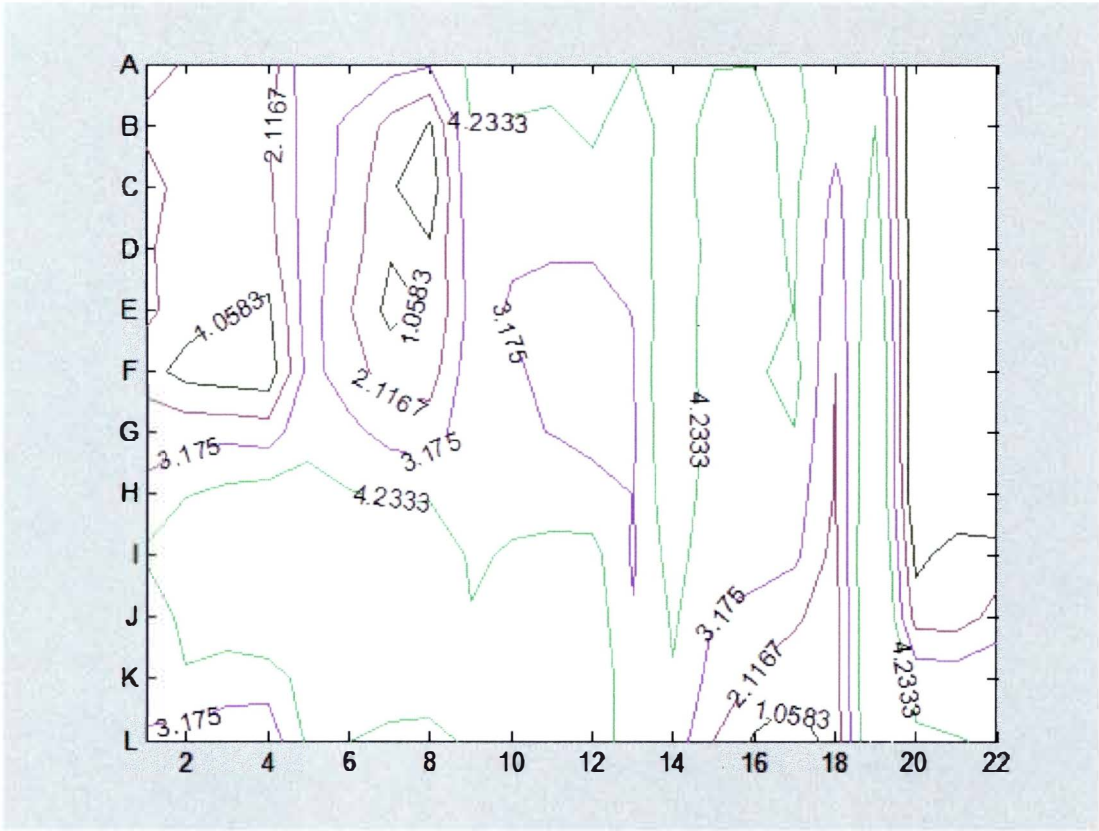

Figure15: Delta E value contour of the comparison between reference and measured data of Kodak08 (grayscale is excluded)

Profiling Scanner Using Reference Data and Measured Data

Three targets were used to create profiles which were Kodak IT8.7/2-1993 1997:08 (specified as Kodak08 in the thesis), Agfa IT8.7/2-1993 1999:03 (C90450XX) (specified as Agfa), and Fuji Film IT8.7/2-1993 2000:05 (specified as Fuji). Commercial profile software used are Monaco Profiler 4.5 (specified as Monaco) and Gretag ProfileMaker 4.1.5 (specified as Gretag).

In the following parts of this thesis, the target used to create a profile is called the training target, and the target used to test a profile is called the testing target.

Three targets were scanned at the same setting as mentioned in the previous part. In order to compare the consistency of profiling software, two profiles for each target were created by using two profiling software. Table 5 shows the Delta E values of different targets assigned different profiles.

Targets		Agfa		Fuji		Kodak08	
Profiling Software		Gretag	Monaco	Gretag	Monaco	Gretag	Monaco
RMS Delta E	Profile with Measured Data	1.42	3.73	1.08	1.58	1.5	2.58
	Profile with reference Data	1.49	3.34	1.3	1.69	1.28	2.77

Table 5: Profiling software consistency test

The RMS Delta E values of the targets assigned with different profiles are very close. It means that the profiling software have consistent profiling ability of using different data to create profiles. In the following, profiles are created by using the measured data of color targets.

Obviously, two profile software can have a different ability to profile the same device. The comparison is shown in Table 6.

Targets and Profile Software			Delta E			
Testing Targets	Profiling Software	Training Targets	RMS	Maximum	Average	Standard Deviation
Agfa	Gretag	Agfa	1.42	7.41	1.13	0.87
	Monaco	Agfa	3.73	29.39	1.77	3.28
Fuji	Gretag	Fuji	1.08	7.02	0.84	0.67
	Monaco	Fuji	1.58	11.57	1	1.22
Kodak08	Gretag	Kodak	1.5	9.34	1.07	1.05
	Monaco	Kodak	2.58	20.43	1.33	2.21

Table 6: The profile ability of two different profile software —Delta E comparisons

Delta L*s, Delta a*s and Delta b*s have the different contribution to Delta Es and RMS Delta E. The table below shows the difference of RMS Delta L*, RMS Delta a*s and RMS Delta b*s of three testing targets assigned different profiles.

Targets and Profile Software			Delta L*	Delta a*	Delta b*
Testing Targets	**Profiling Software**	**Training Targets**	**RMS**	**RMS**	**RMS**
Agfa	Gretag	Agfa	0.4	0.99	0.94
	Monaco	Agfa	0.54	3.45	1.21
Fuji	Gretag	Fuji	0.35	0.83	0.6
	Monaco	Fuji	0.41	1.36	0.69
Kodak08	Gretag	Kodak	0.46	1.25	0.69
	Monaco	Kodak	0.45	2.31	1.05

Table 7: The profile ability of two different profile software — Delta L, Delta a* and Delta b* comparisons

Data in the Table 6 and Table 7 show that the target assigned profiles created by Monaco Profiler have higher RMS Delta E and RMS Delta a* values. Delta a*s are the largest parts of Delta Es for all these profiles.

The extremely large Delta E patches all appeared in the targets assigned with Monaco profiles. Figure 16, Figure 17, and Figure 18 show the contour of Delta E values of testing targets assigned profiles created by Monaco Profiler.

Figure 16 shows that the highest Delta E values of the Agfa target, which was assigned a profile created by Monaco using Agfa as the training target, is located at L13, and G8. H8, H4, L15, L18 also have higher Delta E values.

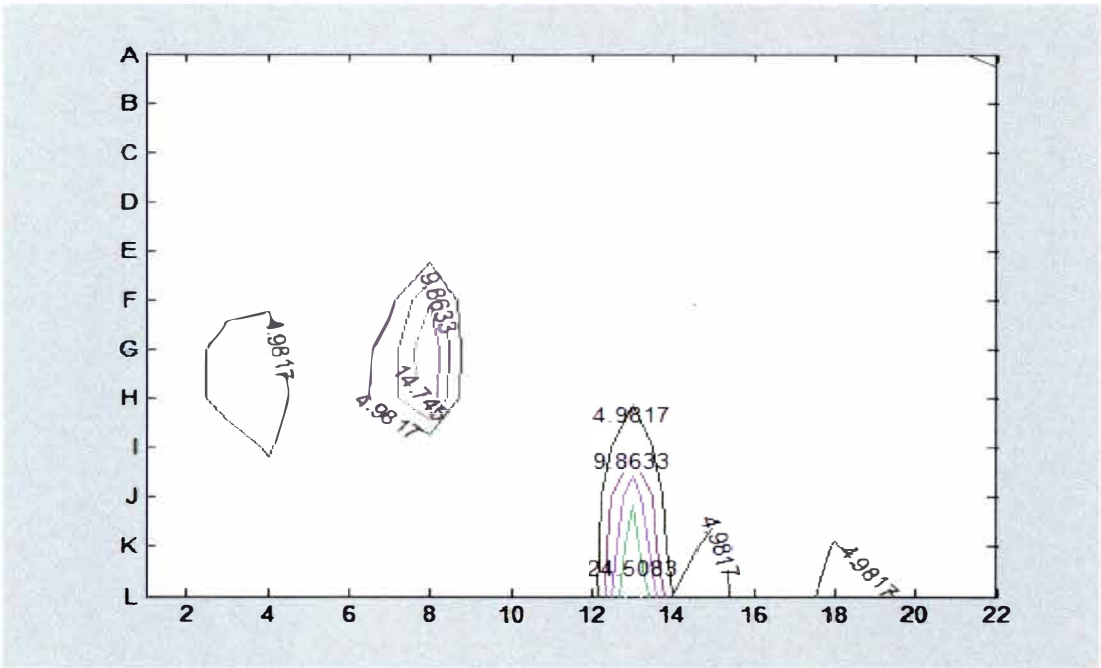

Figure 16: Delta E contour of Agfa target assigned profile created by Monaco Profiler using Agfa as training target (gray scale is excluded)

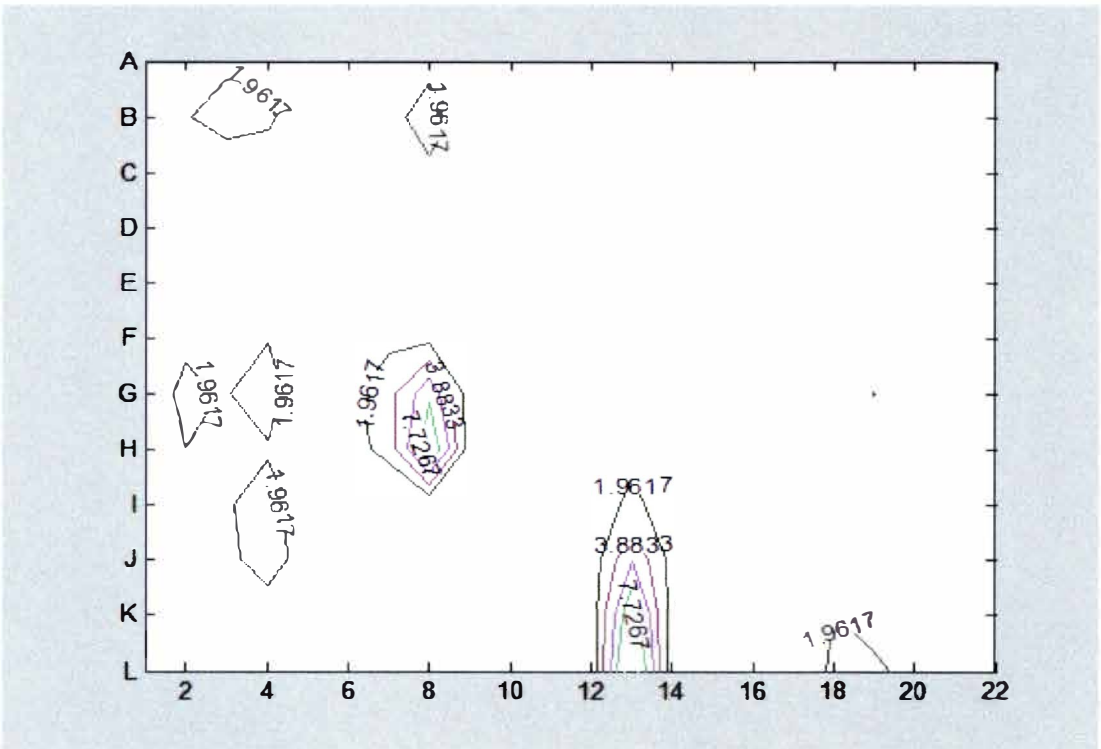

Figure 17: Delta E contour of Fuji target assigned profile created by Monaco Profiler using Fuji as training target (gray scale is excluded)

Figure 17 shows that the highest Delta E of Fuji target, which was assigned profile created by Monaco using Fuji as training target is located at L13. H8 has the second highest Delta E value.

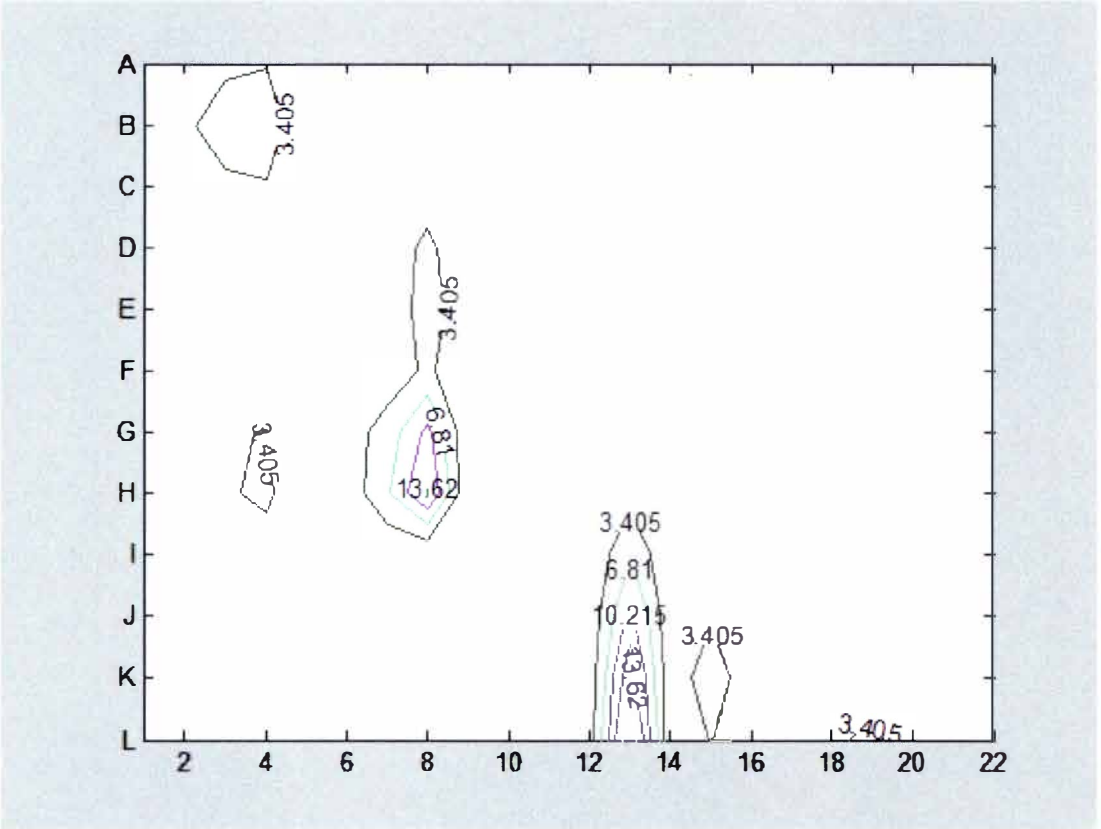

Figure 18: Delta E contour of Kodak08 assigned profile created by Monaco Profiler using Kodak08 as training target (grayscale is excluded)

Figure 18 shows that the highest Delta E values Kodak08, which was assigned a profile created by Monaco using Kodak08 as the training target, is located at L13. H8, E8 and K15 all have higher Delta E values.

The profiles created by Monaco Profiler have the same tendency to generate large Delta E values at L13 and H8 for all manufacturers' targets. Table 8 shows the data of L13 and H8 patches of the three training targets.

Target	ID	Measured Data			Scanned Data(Profiled)			Delta Values			
		LAB_L	LAB_A	LAB_B	LAB_L	LAB_A	LAB_B	Delta L*	Delta a*	Delta b*	Delta E
Agfa	H8	39.97	-29.49	-31.62	41.42	-11.89	-32.11	1.45	17.6	-0.49	17.6
	L13	44.59	-41.06	-36.26	46.1	-11.72	-36.97	1.51	29.3	-0.71	29.3
Fuji	H8	42.36	-33.83	-25.48	43.51	-24.08	-25.38	1.15	9.75	0.1	9.82
	L13	41.83	-38.38	-21.26	43	-26.87	-21.33	1.17	11.5	-0.07	11.5
Kodak 08	H8	40.09	-32.24	-30.21	41.11	-18.51	-30.93	1.02	13.7	-0.72	13.8
	L13	43.8	-39.35	-32.85	45.31	-18.99	-33.62	1.51	20.4	-0.77	20.4

Table 8: Data of the patches have highest Delta E values in three targets which are assigned Monaco profiles

Table 8 shows that Delta a* has the largest contribution to Delta E of all three targets. These patches on the original targets have a similar hue angle h_{ab} around 220° and a similar chroma value C_{ab}*around 43.87. The profiled patches are less saturated than the original ones.

Delta E values of three training targets assigned with profiles created by Gretag ProfileMaker are plotted in contours in Figure 19, 20 and 21 to compare with the targets assigned with profiles created by Monaco Profiler. The highest Delta E values in Figure 19 are located at F7, K16 and G7, and some other patches have relatively higher Delta E values. The Delta E distribution is varied.

Figure 20 shows that the highest Delta E values appear at H7 and G8. L16 also has a higher Delta E value.

In Figure 21, the highest Delta E values are located at L16 and I20. F7, G8 and H7 also have high Delta E values.

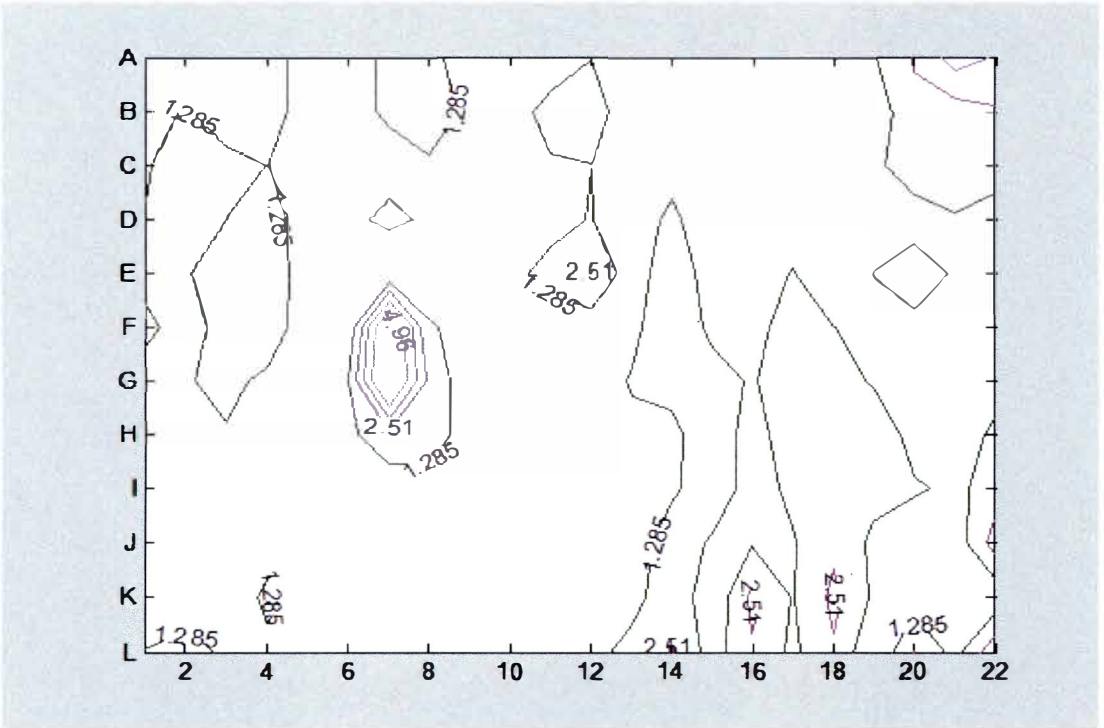

Figure 19; Delta E contour of Agfa assigned profile created by Gretag ProfileMaker using Agfa as training target (grayscale is excluded)

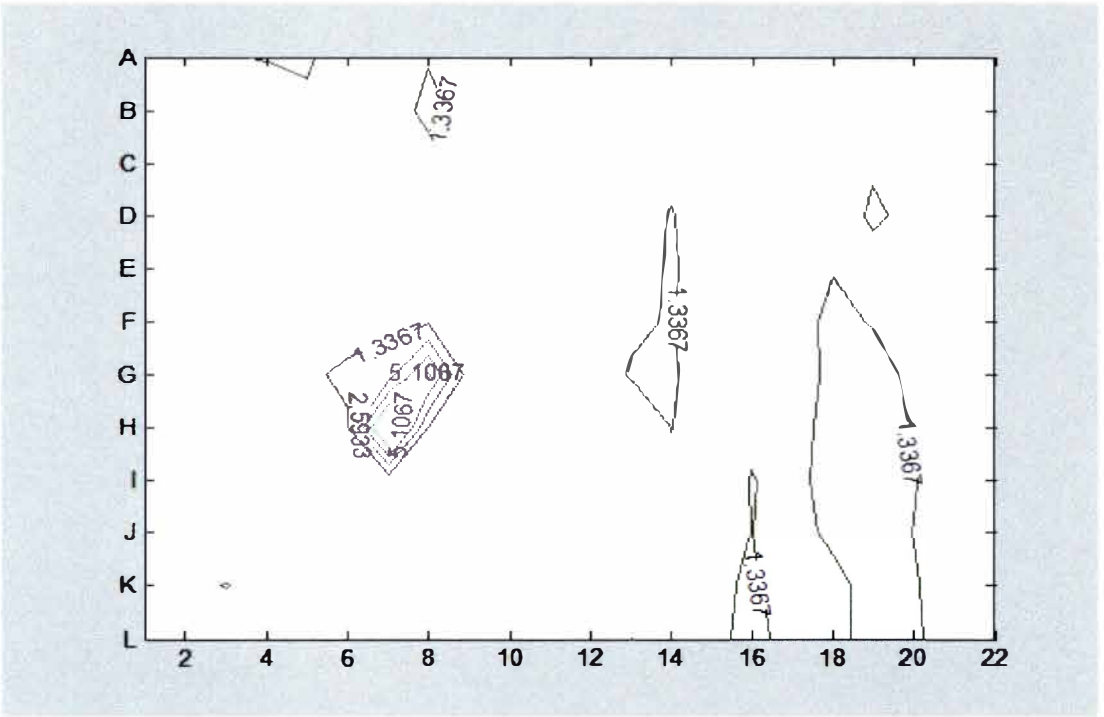

Figure 20: Delta E contour of Fuji target assigned profile created by Gretag ProfileMaker using Fuji as training target (gray scale is excluded)

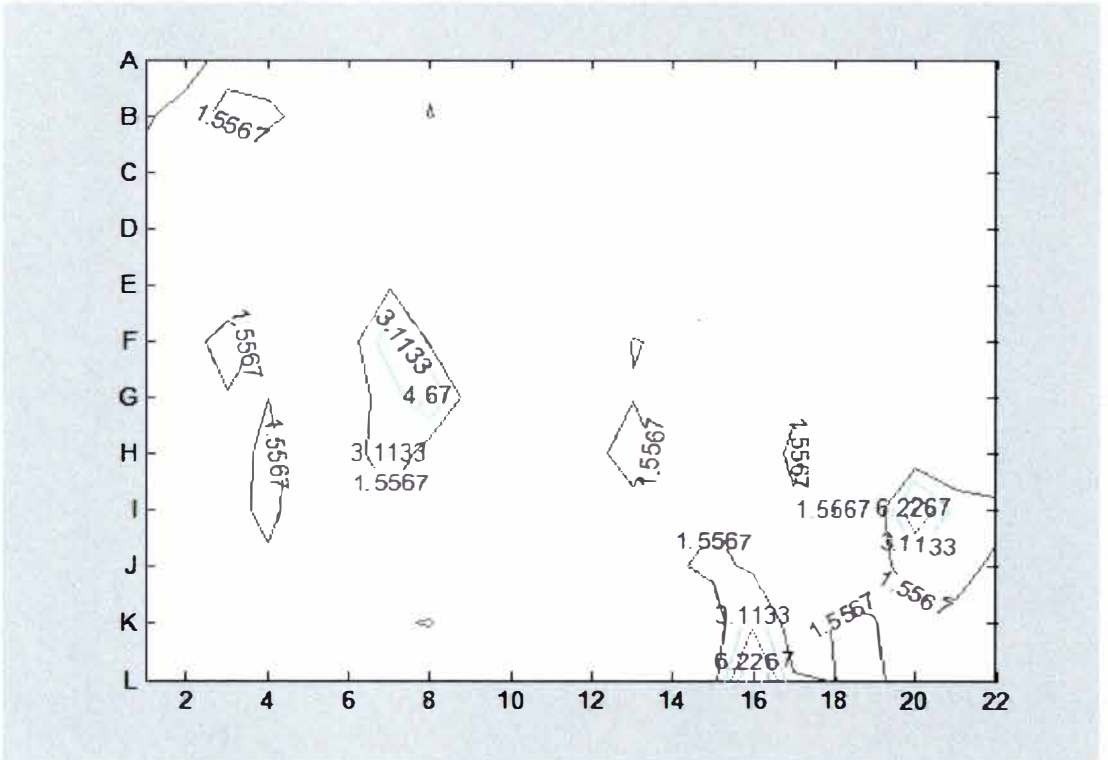

Figure 21: Delta E contour of Kodak08 assigned profile created by Gretag ProfileMaker using Kodak08 as training target (grayscale is excluded)

Unlike the Monaco generated profiles, the highest Delta E values on three targets assigned profiles created by Gretag do not have the same locations. But L16 on three targets assigned profiles created by Gretag all have higher Delta E values, which has the same properties as D_{max} on the grayscale. This match with the Delta E values of D_{max} on grayscales of the testing targets assigned profiles created by Gretag, which also have relative higher values.

The grayscales on the targets can be used to evaluate the ability of profiling software to process the neutral colors. The importance of grayscale balance in color reproduction was discussed by Fleming et al. [20]. Table 9 shows the Delta values of grayscales on each target assigned profiles created by two profiling software using itself as training target.

Table 9 shows that Monaco generated lower RMS Delta E values compared to Gretag, although they are all generally satisfactory. The profiles created by Monaco will be more reliable for reproducing near neutral colors according to the data shown in the table. However, as indicated above, it is less reliable when reproducing some saturated colors.

Targets	Profiling Software	RMS Delta E	RMS Delta L*	RMS Delta a*	RMS Delta b*
Agfa	Gretag	0.97	0.54	0.41	0.69
	Monaco	0.75	0.35	0.59	0.3
Fuji	Gretag	1.13	0.46	0.91	0.47
	Monaco	0.77	0.33	0.61	0.33
Kodak 08	Gretag	2.47	0.39	2.17	0.72
	Monaco	0.76	0.34	0.64	0.23

Table 9: Delta values of grayscale on training targets

The highest Delta Es on the grayscales from the Gretag profile appeared on the patches with lower or higher densities. The highest Delta Es on the grayscales from the Monaco profile appeared only at higher densities.

This showed that profiling software have different abilities to identify and process the near gray colors with higher or lower density. This impacts the ability of these profiles to properly reflect the dynamic range of a scanner.

In the test of this section, six profiles were created by two profiling software using three targets. By calculating Delta values of three targets assigned different profiles, the results showed the different abilities of calibrating and characterizing scanner of profiling software.

Profiles and Targets Cross Testing

Most profiling software users only make one profile with a single profile target. The originals for color reproduction may vary from one major photo paper manufacture to the other. The profile created by one software needs to be tested for accuracy, when assigned to an image printed on different photo paper.

Each of the three targets has two profiles which were created by the two software mentioned above, using measured CIELAB values. Here, the testing targets are assigned profiles other than the one created by themselves to further test the profile accuracy.

Table 10 shows the Delta values of each testing target assigned with different profiles.

Testing Targets and Profile Software			**Delta E**				**Delta L***	**Delta a***	**Delta b***
Testing Targets	**Profiling Software**	**Training Targets**	**RMS**	**Max**	**Average**	**Standard Deviation**	**RMS**	**RMS**	**RMS**
Agfa	Gretag	Fuji	4.76	20.35	3.8	2.88	0.88	3.99	2.54
	Monaco	Fuji	4.27	23.43	3.35	2.65	0.88	3.83	1.68
	Gretag	Kodak08	3.04	9.5	2.64	1.51	0.63	2.55	1.54
	Monaco	Kodak08	3.48	23.78	2.58	2.33	0.54	3.18	1.28
Fuji	Gretag	Agfa	3.99	22.58	3.25	2.32	0.6	3.15	1.81
	Monaco	Agfa	4.15	19.07	3.34	2.46	0.41	3.82	1.56
	Gretag	Kodak08	2.61	14.21	1.97	1.73	0.73	2.28	1.06
	Monaco	Kodak08	2.16	12.1	1.69	1.36	0.5	1.86	0.99
Kodak 08	Gretag	Agfa	3.1	10.2	2.77	1.39	0.46	2.43	1.86
	Monaco	Agfa	4.68	26.35	3.34	3.33	0.51	4.28	1.81
	Gretag	Fuji	3.22	16.02	2.24	2.32	0.8	2.44	1.94
	Monaco	Fuji	3.1	19.98	2.08	2.29	0.83	2.64	1.39

Table 10: Delta values of 3 targets cross testing with different profiles

In the previous test, Monaco had extremely high Delta E values in three targets. In this part, Gretag profiles also generated high Delta E values, over 15. Data in Table 10 show that Delta a*s are slightly higher that Delta L*s and Delta b*s. These also follow the tendency of tests in the previous part.

The contour maps for the cross testing cases show almost the same shapes as the targets assigned profiles created by themselves. This means if the profile is created by Gretag using Agfa target, then this profile assigned to Kodak08, the higher Delta Es appear at almost the same places as they appeared in the Agfa Target. The contour maps of profiles cross testing can be found in the Appendix.

A comparison of grayscale Delta Es, Delta L*s, Delta a*s and Delta b*s on each target are presented in Table 11.

Testing Targets and Profile Software			**Delta E**	**Delta L***	**Delta a***	**Delta b***
Testing Targets	**Profiling Software**	**Training Targets**	**RMS**	**RMS**	**RMS**	**RMS**
Agfa	Gretag	Fuji	3.59	0.83	3.22	1.34
	Monaco	Fuji	4.3	0.94	3.86	1.64
	Gretag	Kodak08	2.33	1.15	1.82	0.88
	Monaco	Kodak08	3.06	0.19	2.72	1.38
Fuji	Gretag	Agfa	4.54	1.04	3.85	2.18
	Monaco	Agfa	3.17	0.46	2.77	1.46
	Gretag	Kodak08	4.1	1.84	3.47	1.18
	Monaco	Kodak08	1.3	0.75	0.96	0.47
Kodak08	Gretag	Agfa	3.41	0.62	2.77	1.89
	Monaco	Agfa	2.32	0.66	1.85	1.27
	Gretag	Fuji	1.94	1.08	1.43	0.74
	Monaco	Fuji	2.21	1.12	1.79	0.64

Table 11: Delta values of grayscales on the targets at cross testing

Compared to Delta values in Table 9, Delta values in Table 11 are much higher. This showed that when the profiles assigned to the targets were different from the profiles created from the target, grayscale reproduction will be less accurate.

Data in Table 10 and 11 show that profiles created by any profiling software using Kodak08 as the training target have relatively lower Delta E values of the entire targets, and grayscales on the targets.

In this part, profiles created by two profiling software were assigned to three targets to cross test. The results showed that when the training targets and testing targets are the same, the profiles produce a relative high profiling quality. When the testing targets are different from training targets, the profiling software did not show large differences of profiling quality.

Additional Profile Accuracy Testing Using R1215 Grayscale

The StoufferR1215 grayscale can also be used to test the accuracy of reproducing neutral colors. The scanned R1215 grayscale was assigned all the profiles that created by Gretag and Monaco profiling software. The Delta values are listed in Table 12.

Profiling Software	**Gretag ProfileMaker**			**Monaco Profiler**		
Training Targets	Agfa	Fuji	Kodak08	Agfa	Fuji	Kodak08
RMS DeltaE	3.70	6.88	5.68	4.40	7.17	6.24
Maximum Delta E	4.61	9.62	6.96	6.14	10.36	8.59
Average Delta E	3.63	6.58	5.61	4.19	6.69	6.01
RMS Delta L*	2.11	2.87	1.86	2.14	2.65	2.16
RMS Delta a*	2.62	5.54	4.70	3.45	6.03	5.23
RMS Delta b*	1.54	2.90	2.61	1.68	2.84	2.64
Standard Deviation of Delta E	0.75	2.09	0.96	1.40	2.71	1.79

Table 12: Delta values of R1215 grayscale

Profiles created by any software using Agfa as the training target have relatively lower Delta E values on the R1215 grayscale. RMS Delta Es and RMS Delta b*s are all of the same magnitude. Again, RMS Delta a*s are higher. The RMS Delta E values on R1215 are higher than the RMS Delta E values on the targets.

Assuming that C* of a real neutral gray is zero, Delta C* can be calculated by using equation (22). Table 13 shows the RMS Delta C* values of grayscales on three targets and the R1215 grayscale.

Target	Agfa	Fuji	Kodak08	R1215
RMS Delta C*	2.17	3.60	2.56	1.03

Table 13: RMS C* of grayscale on three targets and R1215 grayscale

The RMS Delta C* value of grayscale on the Agfa target is the smallest among the three targets. When the profile created using the Agfa target assigned to the R1215 grayscale, the RMS Delta E is the smallest as well. Following the same tendency, the profile created by using the Fuji target assigned to R1215 generates the highest RMS Delta E.

Results in this part showed that the way profiling software processing neutral colors on the training targets effects the quality of profiles processing real neutral gray colors. According to the results in Table 9, profiles can produce very close CIELAB values of grayscales on targets compared with the measured data. But this profile can not produce the same result when assigned to other grayscales on other targets, which have different CIELAB values and different optical properties.

Profile Accuracy Testing Using Targets From the Same Manufacturer With a Different Manufacturing Date

Different photo paper manufacturers use different photo paper and emulsions, which have different properties to reproduce color. One manufacturer may have more than one color target available. This helps to test the accuracy of profiles when assigned to the targets that are from the same manufacturer but with a different manufacturing date.

Kodak testing targets manufactured at different date were tested. We have access to Kodak IT8.7/2-1993 1997:08 (specified as Kodak08) and Kodak IT8.7/2-1993 1997:04 (specified as Kodak04). The Delta values are listed in Table 14.

Data show that the profiles created by Monaco Profiler have higher Delta values than those of Gretag ProfileMaker. When cross testing, profiles using Kodak08 have lower Delta values then Kodak04.

Cross Testing			Delta E				Delta L*	Delta a*	Delta b*
Testing Targets	**Profiling Software**	**Training Targets**	**RMS**	**Maximum**	**Average**	**Stvd.**	**RMS**	**RMS**	**RMS**
Kodak 08	Gretag	Kodak08	1.5	9.34	1.07	1.05	0.46	1.25	0.69
	Monaco	Kodak08	2.58	20.43	1.33	2.21	0.45	2.31	1.05
	Gretag	Kodak04	3.6	14.62	2.57	2.53	1.43	2.58	2.06
	Monaco	Kodak04	4.03	19.42	2.77	2.93	1.36	3.13	2.14
Kodak 04	Gretag	Kodak04	1.3	5.34	1.05	0.77	0.46	1.02	0.67
	Monaco	Kodak04	2.31	18.98	1.32	1.9	0.54	2.01	1.02
	Gretag	Kodak08	2.49	12.8	1.94	1.57	1.13	1.7	1.44
	Monaco	Kodak08	3.35	19.91	2.27	2.47	1.35	2.68	1.5

Table 14: Delta values of cross testing Kodak08 and Kodak04

Delta values of grayscales on Kodak08 and Kodak04 are calculated and shown in Table 15.

Testing Targets and Profile Software			Delta E	Delta L*	Delta a*	Delta b*
Testing Targets	Profiling Software	Profile Assigned	RMS	RMS	RMS	RMS
Kodak 08	Gretag	Kodak 08	2.47	0.39	2.17	0.72
	Monaco	Kodak 08	0.76	0.34	0.64	0.23
	Gretag	Kodak04	1.94	1.08	1.43	0.74
	Monaco	Kodak04	2.21	1.12	1.79	0.64
Kodak 04	Gretag	Kodak04	1.16	0.54	0.93	0.42
	Monaco	Kodak04	1.15	0.59	0.88	0.44
	Gretag	Kodak08	1.9	1.42	0.63	1.1
	Monaco	Kodak08	3.44	2.28	2.11	1.47

Table 15: Delta values of grayscale on two Kodak targets

Data in Table 15 show that the RMS Delta values of grayscale on two testing Kodak targets are higher when assigned the profile created by Gretag using themselves as training targets. When cross testing, Monaco profiles generated higher Delta Values.

R1215 was used here for evaluating the neutral colors when assigned two different profiles created by using Kodak as training targets. Table 16 shows Delta values.

Delta values in Table 16 are very close. It shows that the two profiles have the same ability to reproduce neutral colors. It also shows that Delta values are higher than data of grayscale on the targets.

The tests of this part show that when using targets from the same family as training targets, profiling software can create profiles with similar qualities. When

cross testing, the Delta values are higher, but they are of the same magnitude as well. Monaco generated higher Delta Es when cross testing.

Profiling Software	Gretag		Monaco	
Training Targets	Kodak08	Kodak04	Kodak08	Kodak04
RMS DeltaE	5.68	5.81	6.24	5.62
Maximum Delta E	6.96	11.16	8.59	6.31
Average Delta E	5.61	5.47	6.01	5.56
RMS Delta L*	1.86	1.71	2.16	0.94
RMS Delta a*	4.70	4.24	5.23	4.87
RMS Delta b*	2.61	3.58	2.64	2.63
Standard Deviation of Delta E	0.96	2.04	1.79	0.83

Table 16: Delta values of R1215 grayscale assigned profiles created by using Kodak targets

Further Testing by Using Different Scanners

The distribution of Delta values on the targets may vary when the targets are scanned with different scanners. The responding of CCD sensors are different from one scanner to the other. The R, G, B values of each patch will be different. When the scanned target is used as the training target, the quality of profiles will be different as well.

The scanner used for further testing was a UMAX Astra 4000U. The Kodak08 was used as the training target. The Kodak04 target was scanned at the same setting for comparison.

R1215 was used to test the dynamic range and gray balance of the scanner.

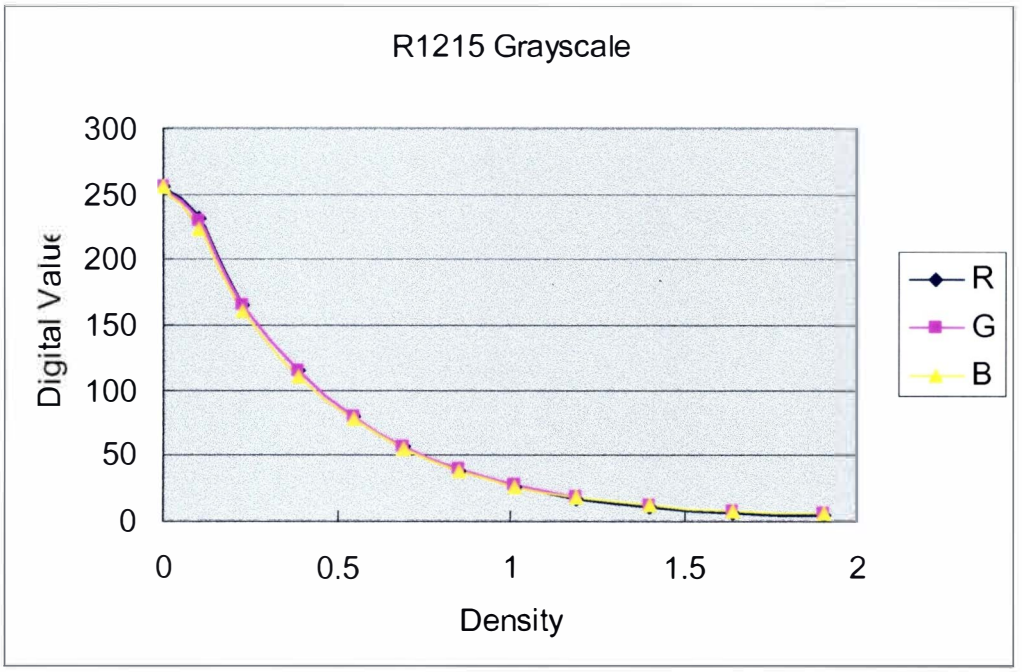

Figure 22: RGB digital values of Stouffer R1215 grayscale scanner by UMAX Astra 4000U with no auto adjustment

Figure 22 shows that the UMAX Astra 4000U has a high dynamic range and good gray balance especially in shadow areas compared with the HP Scanjet 7400C.

Two profiles were created by Monaco and Gretag using Kodak08 as the training target. The profiles were assigned to Kodak08 and Kodak04. Table 17 shows the Delta values of the entire targets.

Cross Testing			Delta E			
Testing Targets	**Profiling Software**	**Training Targets**	**RMS**	**Maximum**	**Average**	**Standard Deviation**
Kodak 08	Gretag	Kodak08	1.77	4.88	1.42	1.05
	Monaco	Kodak08	1.96	7.64	1.45	1.32
Kodak 04	Gretag	Kodak08	2.12	6.87	1.67	0.81
	Monaco	Kodak08	2.36	7.66	1.75	0.88

Table 17: Delta E values of Kodak08 and Kodak04 assigned profile created by Gretag and Monaco using Kodak08 as training target

Data in Table 17 show that RMS Delta E values of the targets assigned with profiles created by Monaco are slightly higher than the profiles created by Gretag. This follows the same tendency of the targets scanned by the HP Scanjet 7400C. The maximum Delta E values are much lower than the same target scanned by the HP Scanjet 7400C.

Cross Testing			Delta L*	Delta a*	Delta b*
Testing Chart	**Profiling Software**	**Training Targets**	**RMS**	**RMS**	**RMS**
Kodak08	Gretag	Kodak08	1.42	0.58	1.21
	Monaco	Kodak08	0.65	1.28	1.34
Kodak04	Gretag	Kodak08	1.35	1.42	1.32
	Monaco	Kodak08	1.39	1.69	1.59

Table 18: Delta L*, Delta a* and Delta b* values of Kodak08 and Kodak04 assigned profiles created by Gretag and Monaco using Kodak08 as training target

RMS Delta L*s, Delta a*s and Delta b*s are very close in both testing targets. The results shown in the test of HP Scanjet 7400C have higher RMS Delta a* values than RMS Delta L* and RMS Delta b* values.

Testing Targets and Profile Software			Delta E	Delta L*	Delta a*	Delta b*
Testing Targets	**Profiling Software**	**Trainging Targets**	**RMS**	**RMS**	**RMS**	**RMS**
Kodak08	Gretag	Kodak 08	1.99	1.19	1.3	1.19
	Monaco	Kodak 08	0.78	0.35	0.53	0.75
Kodak04	Gretag	Kodak08	1.58	0.88	0.64	1.06
	Monaco	Kodak08	1.56	0.71	1.06	1.09

Table 19: Delta values of grayscales on Kodak08 and Kodak04 assigned profiles created by Gretag and Monaco using Kodak08 as training target

Table 19 shows that the profile created by Monaco is more reliable to reproduce near neutral colors according to the data on the targets. These results have the same tendency as the results of the HP Scanjet 7400C.

Figure 23 shows that the higher Delta E values appear at K16, L19 and F3. These patches which showed the higher Delta E values in Kodak08 target scanned by UMAX Astra 4000U assigned profile created by Gretag profiling software, show in Figure 21 as well.

Figure 24 shows that the higher Delta E values appear at L13, K16, L19, H4 and E8, which also appear in the contour map of Kodak08 scanned by HP Scanjet 7400C assigned the Monaco profile. The higher Delta E values at E3 and E8 in Figure 18 are in Kodak08 scanned by HP Scanjet 7400C as well.

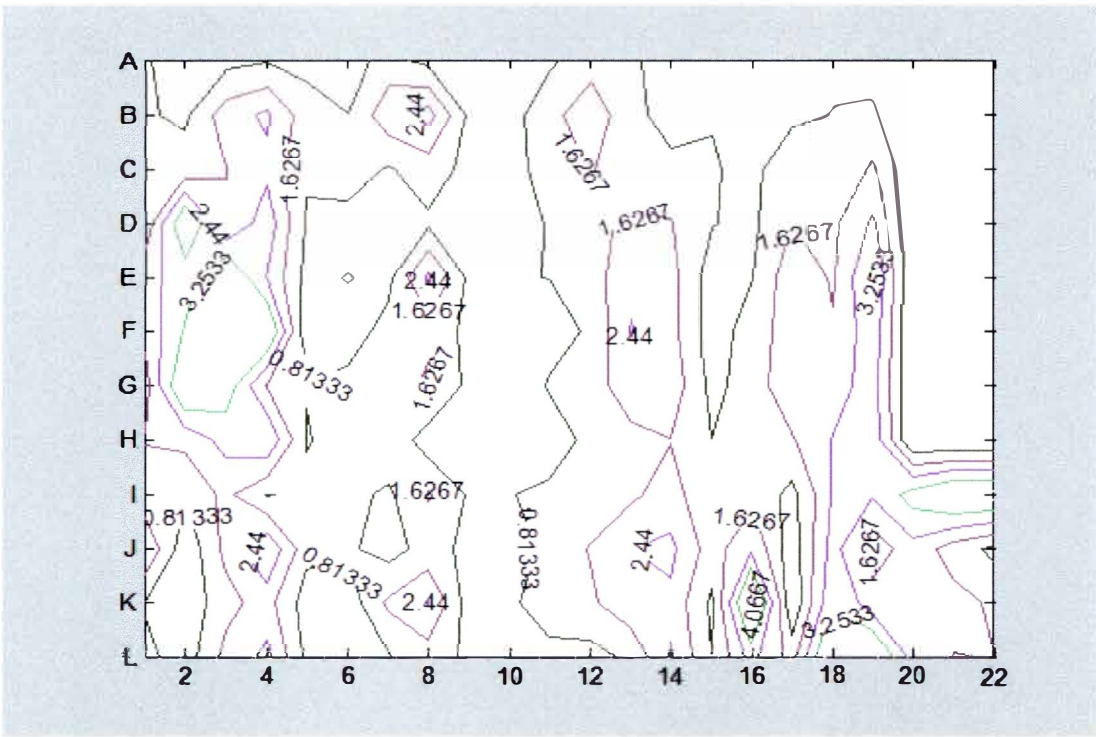

Figure 23: Delta E contour of Kodak08 (scanned by UMAX Astra 4000U) assigned profile created by Gretag ProfileMaker (grayscale is excluded)

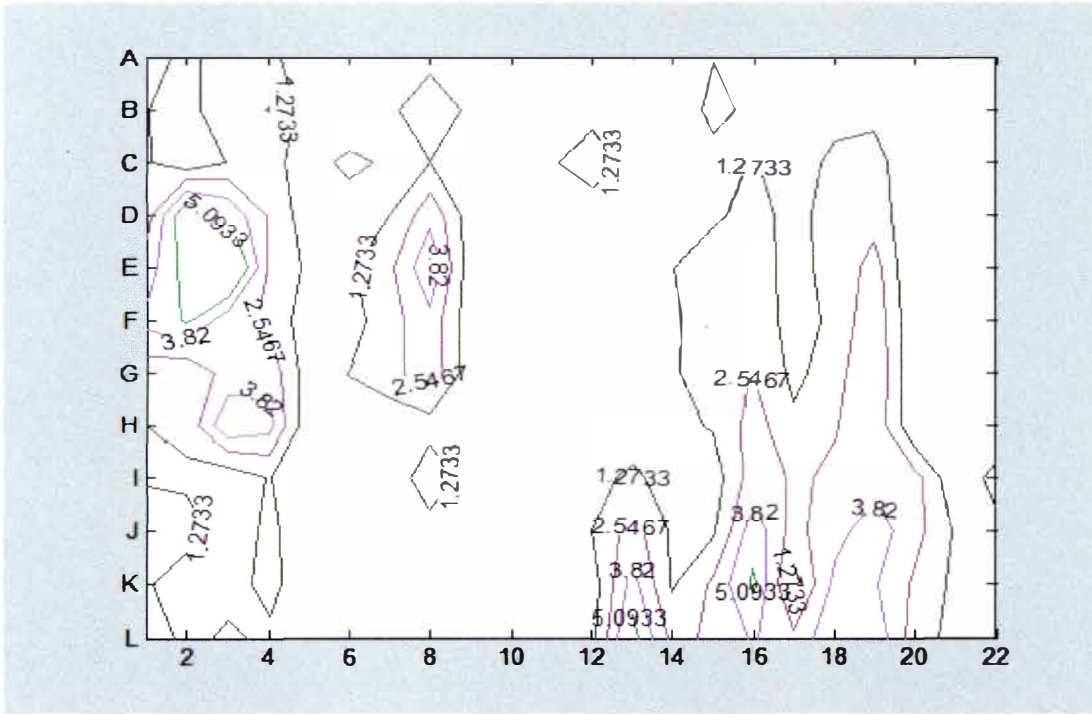

Figure 24: Delta E contour of Kodak08 (scanned by UMAX Astra 4000U) assigned profile created by Monaco Profiler (grayscale is excluded)

R1215 was assigned the profiles to test the ability of reproducing neutral colors.

Profiling Software	Training Targets	RMS Delta E	Maximum Delta E	Average Delta E	RMS Delta L*	RMS Delta a*	RMS Delta b*	Standard Deviation of Delta E
Gretag	Kodak08	7.73	9.89	7.57	2.29	5.06	5.38	1.62
Monaco	Kodak08	8.21	11.21	7.99	1.9	4.8	6.33	2.01

Table 20: Delta values of R1215 grayscale assigned profiles created by Gretag and Monaco

Data in Table 20 show that for the profile created by Monaco is assigned to the R1215 grayscale, the Delta values are higher than the profile created by Gretag. This has the same tendency as R1215 grayscale scanned by HP Scanjet 7400C. RMS Delta a* and RMS Delta b* values are close in the table above.

Compared with the results of targets scanned by HP Scanject 7400C, the results of targets scanned by UMAX Astra 4000U are relative better in terms of RMS Delta E values of entire targets. RMS Delta a* values are smaller for targets scanned by UMAX Astra 4000U compared to those scanned by HP Scanjet 7400C. This can be related to quality of scanners which can affect the profiling quality.

CONCLUSIONS

The experiments described in this thesis provide methods of quantitative analysis of profile quality. Standard color targets were used to create profiles. Profile quality can be compared by using the color difference, Delta E. For neutral colors, Delta L*, Delta a* and Delta b* are very useful. For chromatic patches on standard targets, C* is a useful parameter.

Profiling software has a varying ability to profile one scanner when using different color targets as training targets. Although the standard of IT8.7/2-1993 describes color patches in chroma hue angle and lightness, every target manufactured by different photo paper with different emulsion has a different CIELAB values. These differences result in differences in response of profiling software.

The accuracy of scanners, especially the special sensitivity of CCD sensors is also important for profiling software to create accurate profiles.

The profile quality for two profiling software is generally acceptable. The difference between the two software is the way they process the chroma and neutral colors. Basically, profiling software can generate more accurate profile by using the target scanned by a well gray balanced scanner.

The RMS Delta E becomes minimal when the testing target is the same as the training target. When the testing target is different from the training target, the RMS

Delta E is about three to four times larger than the RMS Delta E of the training target. The RMS Delta E values show that when cross testing, the qualities of profiles do not have large difference. The profile performs better if the training target and testing target are from same family.

The Monaco Profiler usually generates higher Delta E values at highly saturated cyan, blue and some green patches, which have the same chromas or hue angles. The Gretag ProfileMaker always generates higher Delta E values at Dmax of grayscales. These patches appeared on all the testing targets no matter which targets or scanners were chosen.

For two profiling software, L*s are easier to process and a*s have the highest difference. All the testing targets showed that the profiling software can generate the lowest RMS Delta L* values compared to RMS Delta a* and RMS Delta b* values.

Both profiling software can approach CIELAB values of grayscale to reference or measured data on any training target. When profiles assigned to the standard grayscale which is more neutral than the grayscales on targets, the RMS Delta E is much higher than the RMS Delta Es of the grayscales on the targets. This shows that profiling software has a limited ability to identify and process real neutral colors. RMS Delta Es of neutral grayscales depend on the chromatic values of the training targets. When the training target has lower chromatic values on grayscale, the profile created is better for producing neutral colors. If the grayscale on the target is closer to neutral, the profile created by that target has higher accuracy in reproducing neutral colors.

Scanner quality also affects profile quality. The better the gray balance of the scanner brings the better overall profiling quality.

Profiling software needs to be improved in processing real neutral colors and highly saturated colors.

APPENDIX A

Delta E Contour Maps

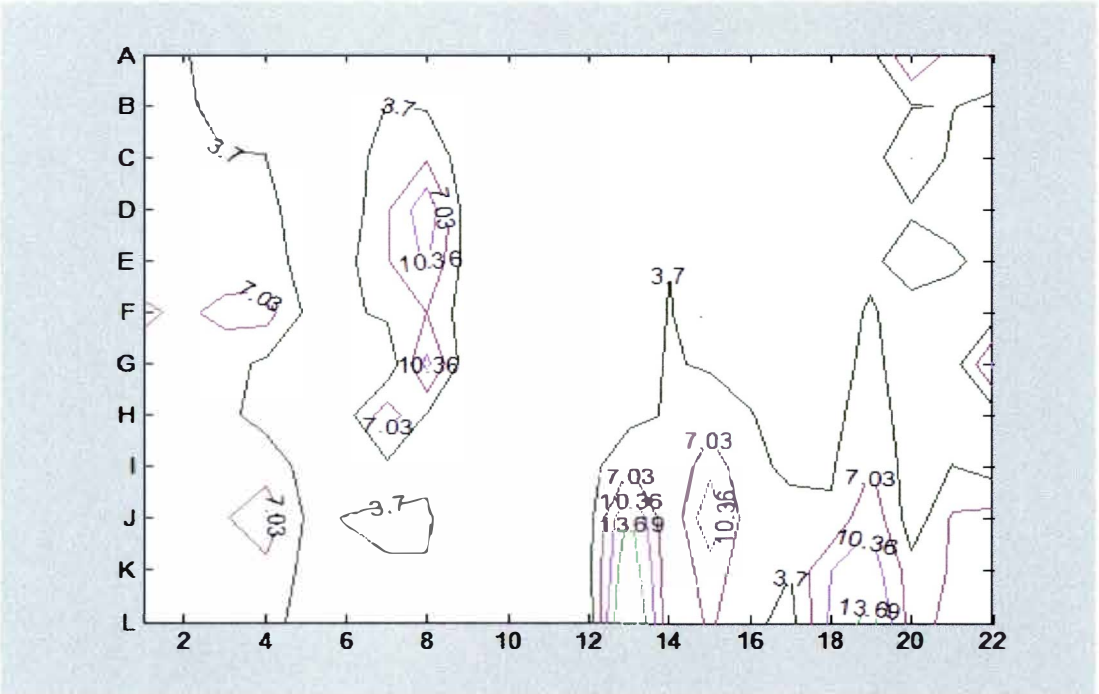

Figure 25: Delta E contour of Agfa assigned profile created by Gretag ProfileMaker using Fuji as training target (grayscale is excluded)

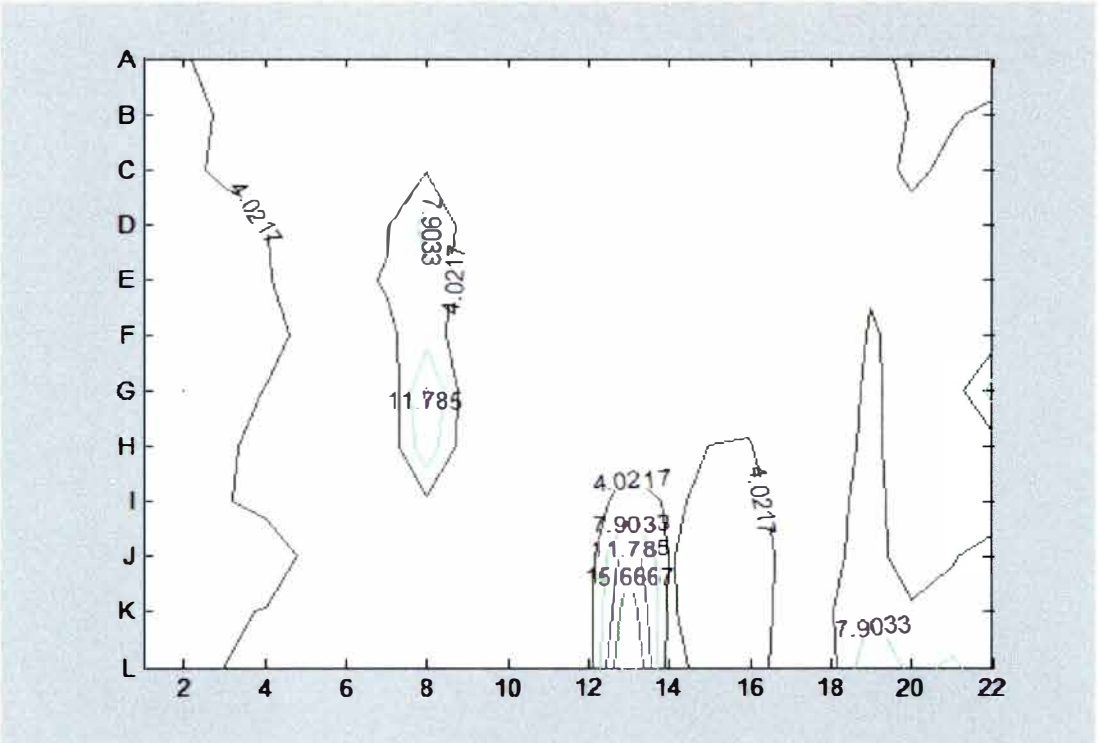

Figure 26: Delta E contour of Agfa assigned profile created by Monaco Profiler using Fuji as training target (grayscale is excluded)

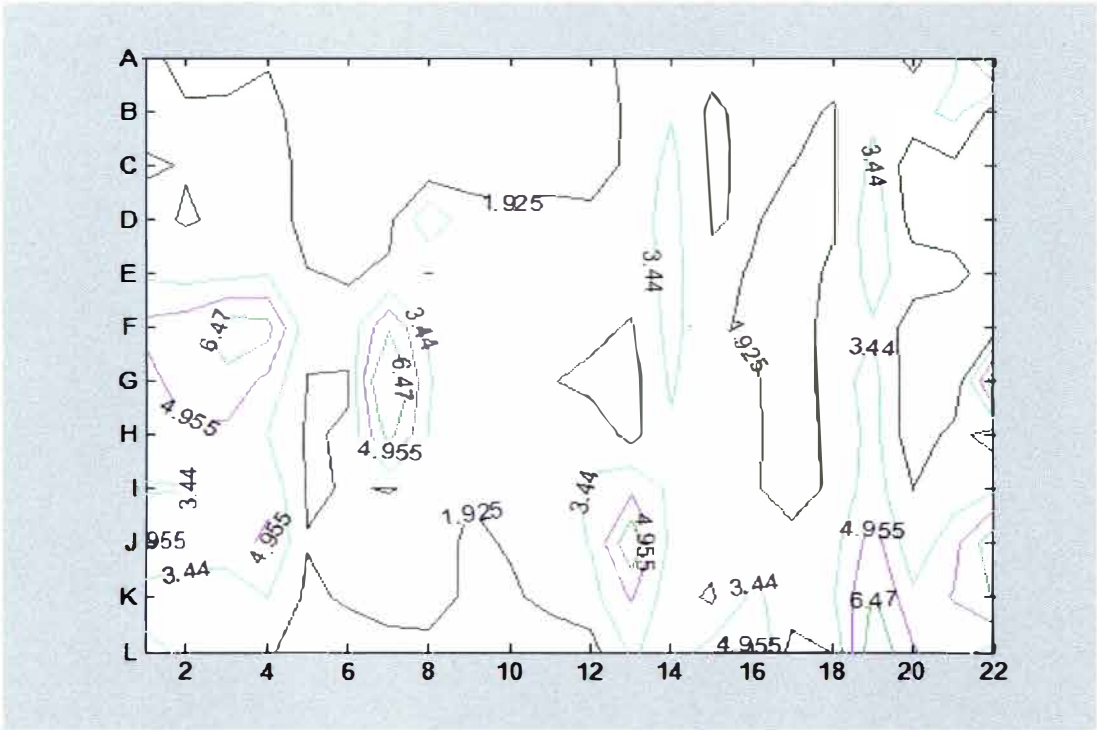

Figure 27: Delta E contour of Agfa assigned profile created by Gretag ProfileMaker using Kodak08 as training target (grayscale is excluded)

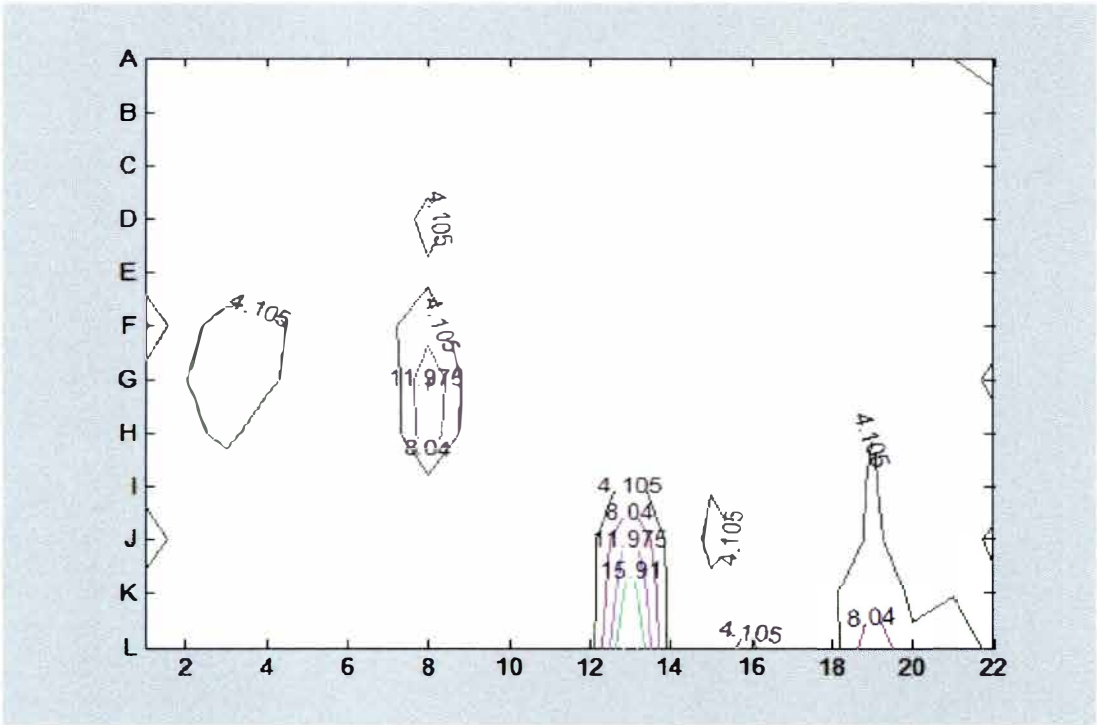

Figure 28: Delta E contour of Agfa assigned profile created by Monaco Profiler using Kodak08 as training target (grayscale is excluded)

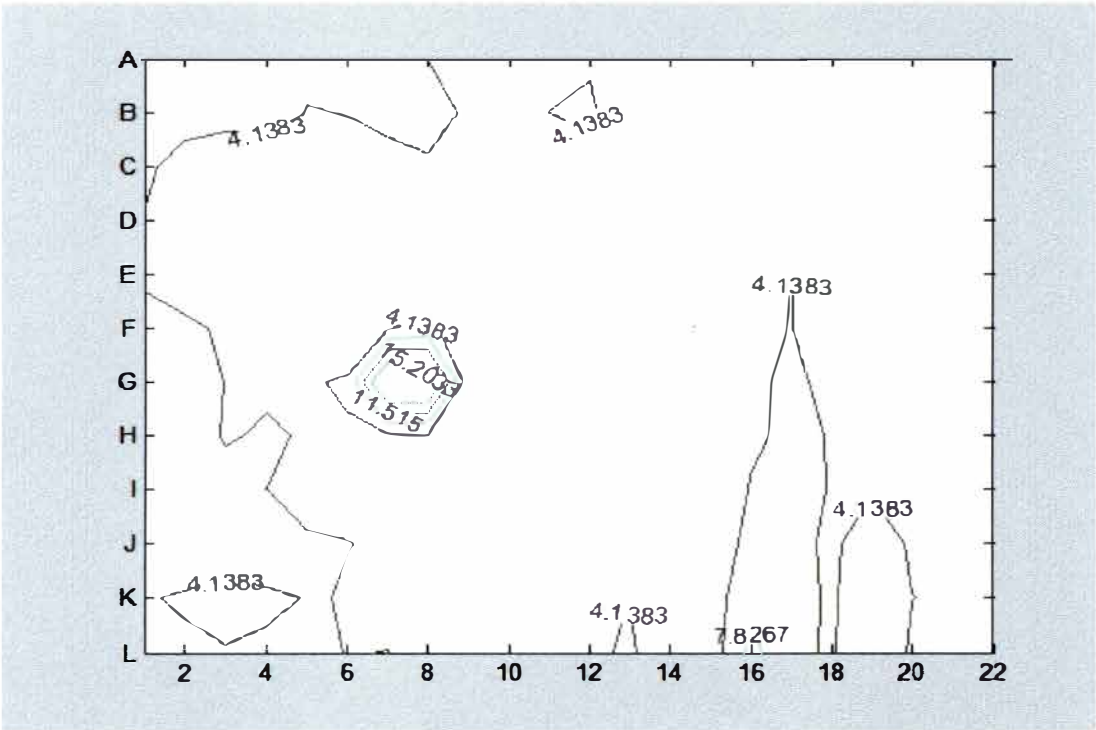

Figure 29: Delta E contour of Fuji assigned profile created by Gretag ProfileMaker using Agfa as training target (grayscale is excluded)

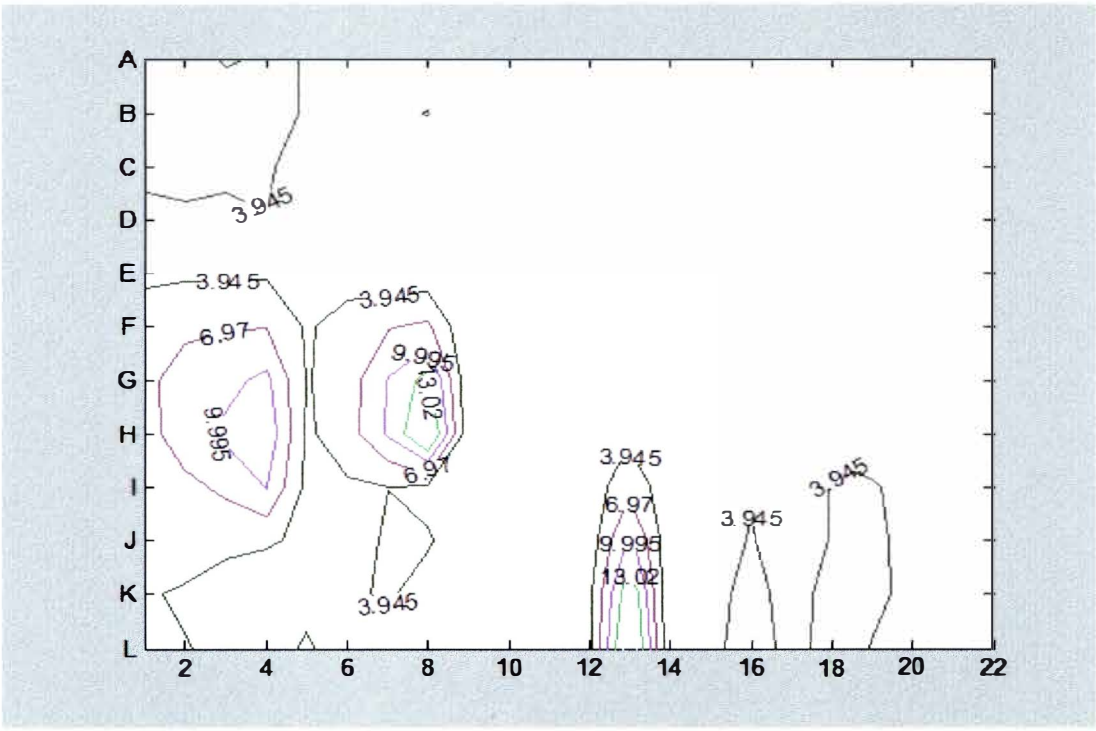

Figure 30: Delta E contour of Fuji assigned profile created by Monaco Profiler using Agfa as training target (grayscale is excluded)

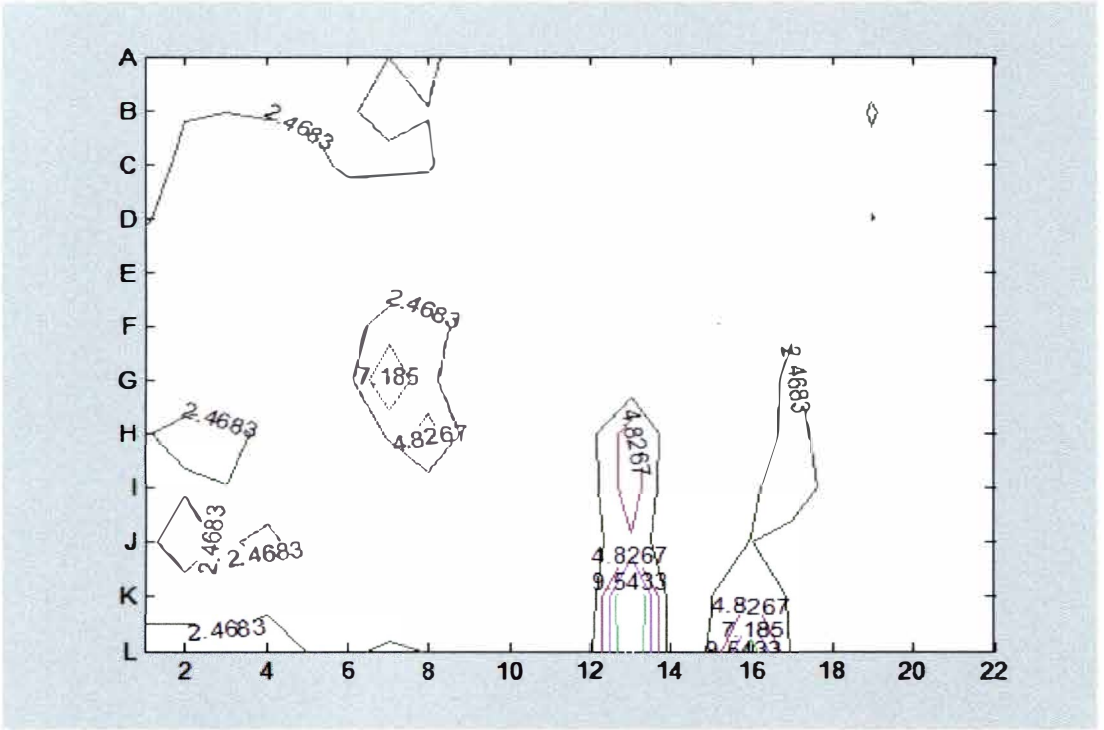

Figure 31: Delta E contour of Fuji assigned profile created by Gretag ProfileMaker using Kodak08 as training target (grayscale is excluded)

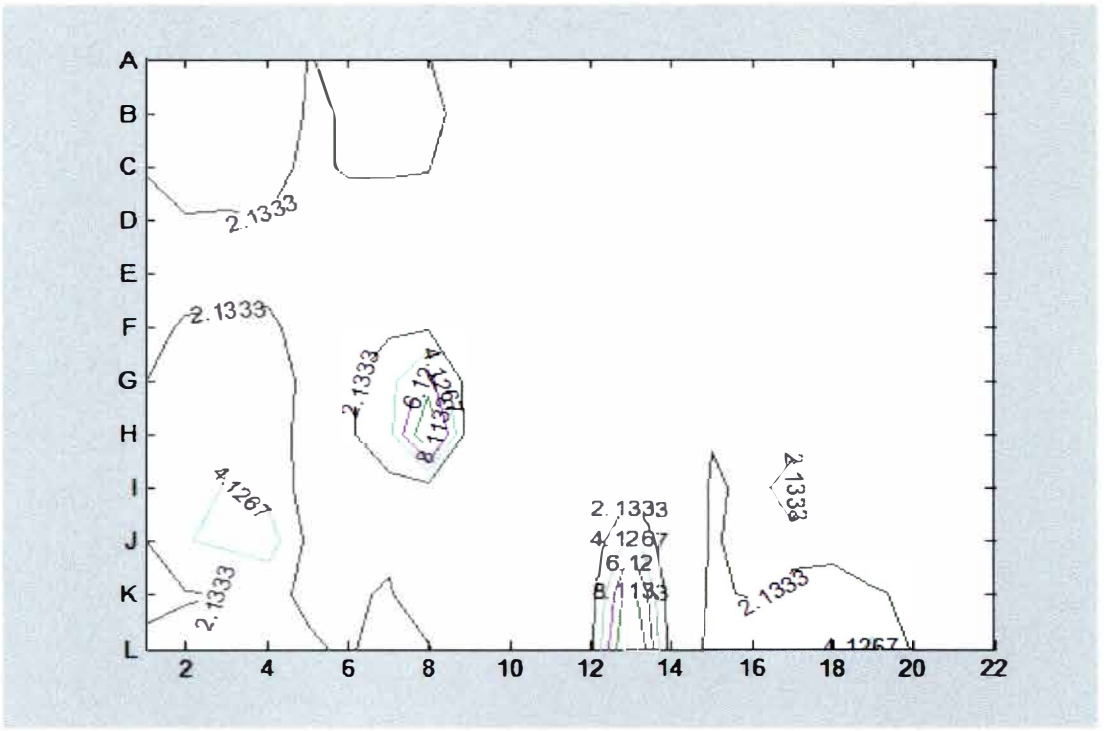

Figure 32: Delta E contour of Fuji assigned profile created by Monaco Profiler using Kodak08 as training target (grayscale is excluded)

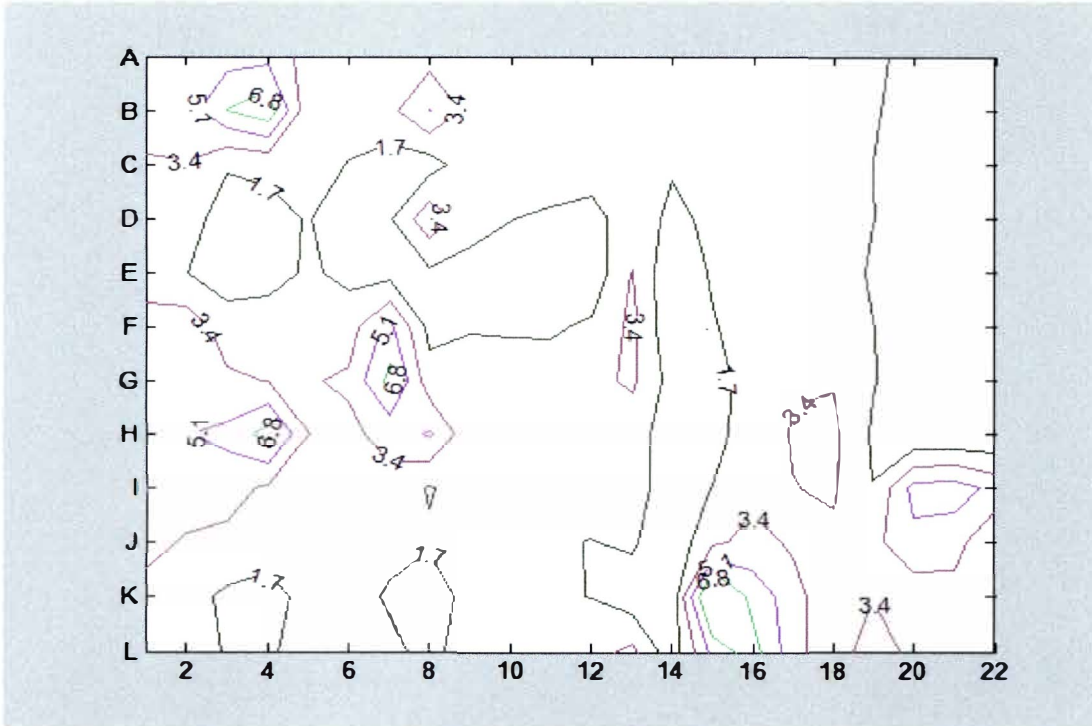

Figure 33: Delta E contour of Kodak08 assigned profile created by Gretag ProfileMaker using Agfa as training target (grayscale is excluded)

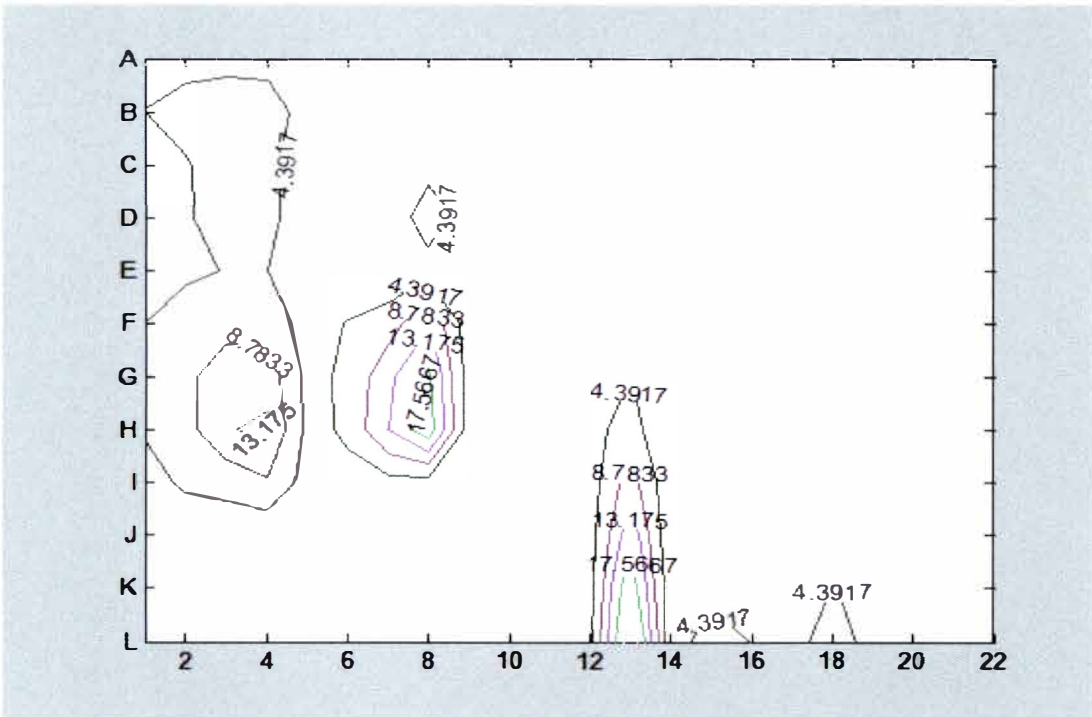

Figure 34: Delta E contour of Kodak08 assigned profile created by Monaco Profiler using Agfa as training target (grayscale is excluded)

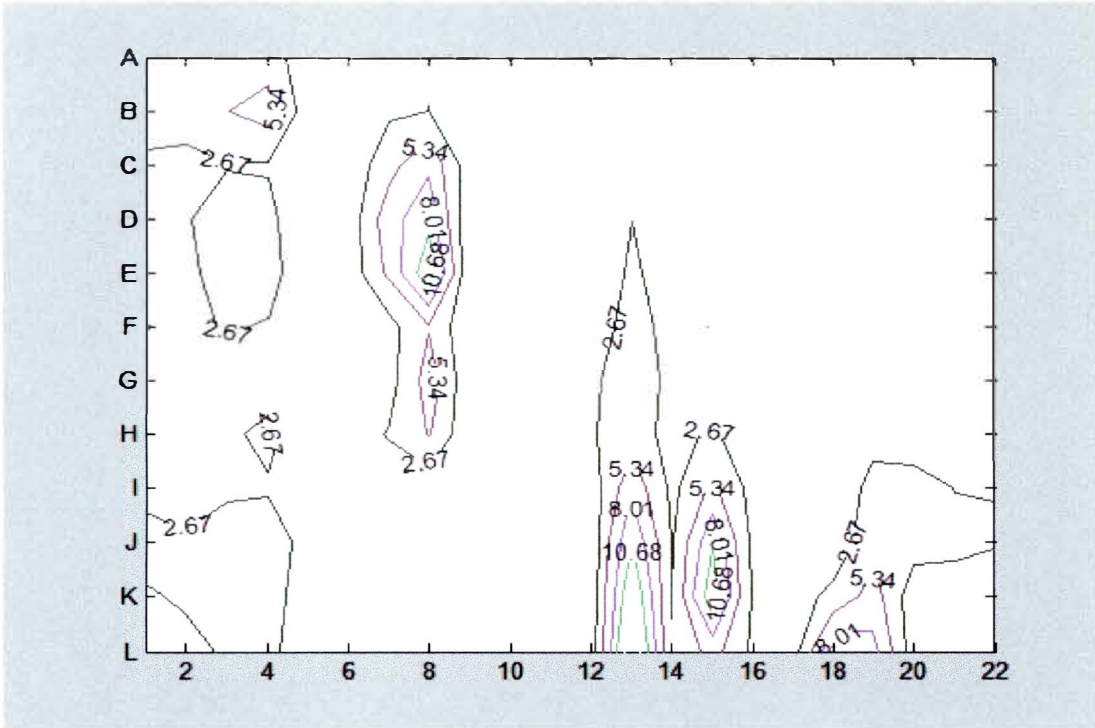

Figure 35: Delta E contour of Kodak08 assigned profile created by Gretag ProfileMaker using Fuji as training target (grayscale is excluded)

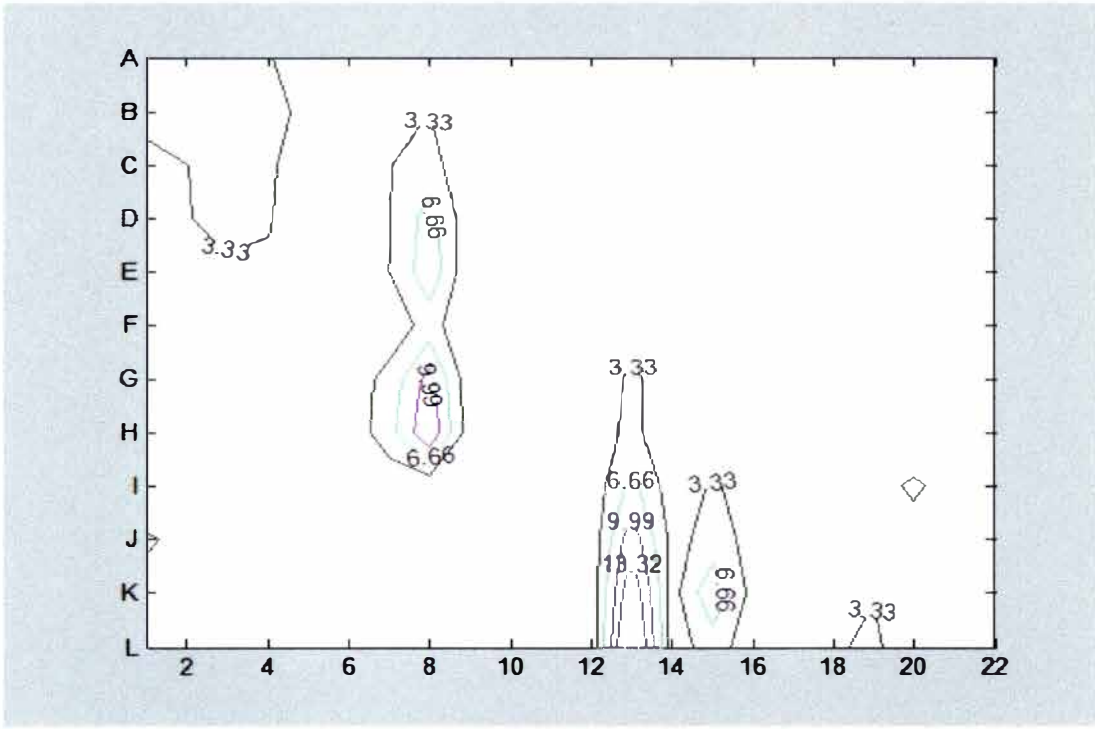

Figure 36: Delta E contour of Kodak08 assigned profile created by Monaco Profiler using Fuji as training target (grayscale is excluded)

BIBLIOGRAPHY

1. Richard M. Adams II, Joshua B. Weisberg, "The GATF Practical Guide to Color Management", GATF Press, Second Edition, 2000
2. Abhay Sharma, "Understanding Color Management", Thomson Delamar Learning, 2004
3. LaserSoft Imaging, SilverFast Manual, Chapter 7 "Color Management", 2001.
4. Rafael C. Gonzalez, Richard E. Woods, "Digital Image Processing", 2nd Edition, Addison-Wesley Pub Co., January, 2002
5. Roy S. Berns, Munsell Color Science Laboratory Technical Report, "The Science of Digitizing Two-Dimensional Works of Arts for Color-Accurate Image Archives-Concept Through Practice", 2000.
6. Commission Internationale de l'Eclairage (CIE) Proceedings 1931, Cambridge University Press, Cambridge, 1932
7. CIE Publication No. 15, Supplement Number 2 (El. 3.1): Official Recommendations on Uniform Color Spaces, Color-Difference Equations, and Metric Color Terms. Commission Internationale de L' Eclairge, 1976
8. Henryk Palus. "Colour Space", 1st Edition, Chapmann and Hall, 1998.
9. P. Laden, "Chemistry and Technology of Water Based Inks", Chapter 2, "Colorimetry and the Calculation of Color Difference", Blackie Academic and Professional, 1997.
10. Roy S. Berns, "Billmeyer and Saltzamn's Principles of Color Technology", 3rd Edition, John Wiley &Sins, Inc., 2002
11. CIE No. 116, "Industrial Colour Difference Evaluation", Commission Internationale de l'Eclairage, Vienna, Austria 1995

12. Myrna Penny, "Colour Management for a Digital World", Canadian Printer, June 1997
13. International Color Consortium, "Specification ICC.1:2002-12, File Format for Color Profiles (Version 4.0.0)", 2001
14. G.Holst, "CCD Arrays, Cameras, and Display", 2nd ed. Intl. Soc. for Optical Eng., Bellingham, WA,1998
15. Gaurav Sharma, H. Joel Trussell, "Digital Color Image", IEEE Transaction on Image Processing, vol. 6, No. 7, July 1997
16. Massimo Mancuso, "An Introduction to the Digital Still Camera", ST Journal of System Research, vol. 2, December 2001
17. Tony Johnson, "Methods for characterizing Colour Scanners and Digital Cameras", "Colour Engineering" John Wiley & Sons, Ltd. 2002
18. ANSI IT8.7/2:1993 Graphic Technology- Color Reflection Target for Input Scanner Calibration (incorporated in ISO 12641)
19. ANSI IT8.7/1:1993 Graphic Technology- Color Transmission Target for Input Scanner Calibration (incorporated in ISO 12641)
20. Paul D. Fleming, Holly Jewell and Aniruddha D. Khandekar, "The Leverage of Gray Balance in Controlling Perceptual and Quantitative Colorimetry", Journal of Graphic Technology, In Press.
21. Abhay Sharma and Paul D. Fleming, "Measuring the Quality of ICC Profiles and Color-Management Software" Seybold Report, Vol. 2, No. 19 January 13, 2003
22. Abhay Sharma and Paul D. Fleming, "Evaluating the Quality of ICC Color Management Profiles", Proceedings of the 2002 TAGA Annual Technical Conference, Ashville, NC, April 14-17, 2002